Appendix A.32:

Shirley Primary School – CPT 54376

Table 1: Site Description for Shirley Primary School (CC LIQ 15 – CPT 54376).

Attribute	Yes/No			Description/Date	Symbol in Figure 1
	10-m Buffer	20-m Buffer	50-m Buffer		
Near a body of surface water or other free face features?	No	No	No	The center of the site is ~110 m away from the unnamed stream to the SW and ~260 m away from the same stream to the NE. The height of the free face is ~1 m.	NA
Lateral spreading observed during the CES?	No	No	No	No lateral spreading was observed by the mapping team.[1]	NA
Nearby buildings or structures?	No	Yes	Yes	Buildings cover 1% and 16% of the 20-m and 50-m buffers, respectively. They are in the NW, SW, and SE quadrants of the 50-m buffer and the SW quadrant of the 20-m buffer.	White Fill + Brown Outline
Sloping land?	No	No	No	Flat land, open + school/commercial area.	NA
Step changes in the ground surface?	No	No	No	NA	NA
Retaining walls?	No	No	No	NA	NA
Vegetation?	Yes	Yes	Yes	Trees and bushes cover 43, 41, and 17% of the 10-, 20-, and 50-m buffers, respectively. They are in the W portion of the 10-m buffer, NW, SW, and SE quadrants of the 20-m buffer, and all quadrants of the 50-m buffer.	White Fill + Green Outline
Anthropogenic changes to the site between the LiDAR surveys?	Yes	Yes	Yes	Earthwork in the SE quadrant of all buffers between Apr 2005 and Jan 2006. Two goals and a pitch were added to the N portion of the 50-m buffer between Jan 2006 and Mar 2009. Pavement in the W portion of all buffers was removed between Mar 2009 and Sep 3, 2010. Pavement in all quadrants of all buffers was painted as a sports court between Sep 5, 2010 and Feb 7, 2011 (new pavement is unlikely). Earthwork in the N portion of the 20- and 50-m buffers, new pavement in all quadrants of all buffers, and veget. removal in the W portion of all buffers between Feb 26, 2011 and Mar 28, 2011. Building removal in the SW quadrant of the 50-m buffer and veget. removal in the W portion of all buffers between Mar 28, 2011 and Aug 30, 2011. Building addition in the W portion of the 20- and 50-m buffers and re-grassing in the N portion of the 20- and 50-m buffers between Apr 2012 and Oct 2012. Building addition in the NE quadrant of the 50-m buffer between Mar 2013 and Aug 2013. Building addition in the NE quadrant of the 20- and 50-m buffers between Aug 2013 and Jan 2014. Veget. removal in the NW quadrant of the 20- and 50-m buffers between Jan 2015 and Jun 2015. Veget. addition in the NW quadrant of the 20- and 50-m buffers between Sep 2015 and Nov 2015.	Building Removal: Orange Crossline; Vegetation Removal: Green Crossline
Other important factors?	No	No	Yes	Two goals and a pitch are present in the N portion of the 50-m buffer.	Goal/Pitch: Orange Outline

Note: Buffer is the area within a circle of a specified radius with CPT investigations done at its center (172.653071°, -43.507478°).

[1] Canterbury Geotechnical Database. (2012). "Observed Ground Crack Locations", Map Layer CGD0400 - 23 July 2012, retrieved July 09, 2018 from https://canterburygeotechnicaldatabase.projectorbit.com/

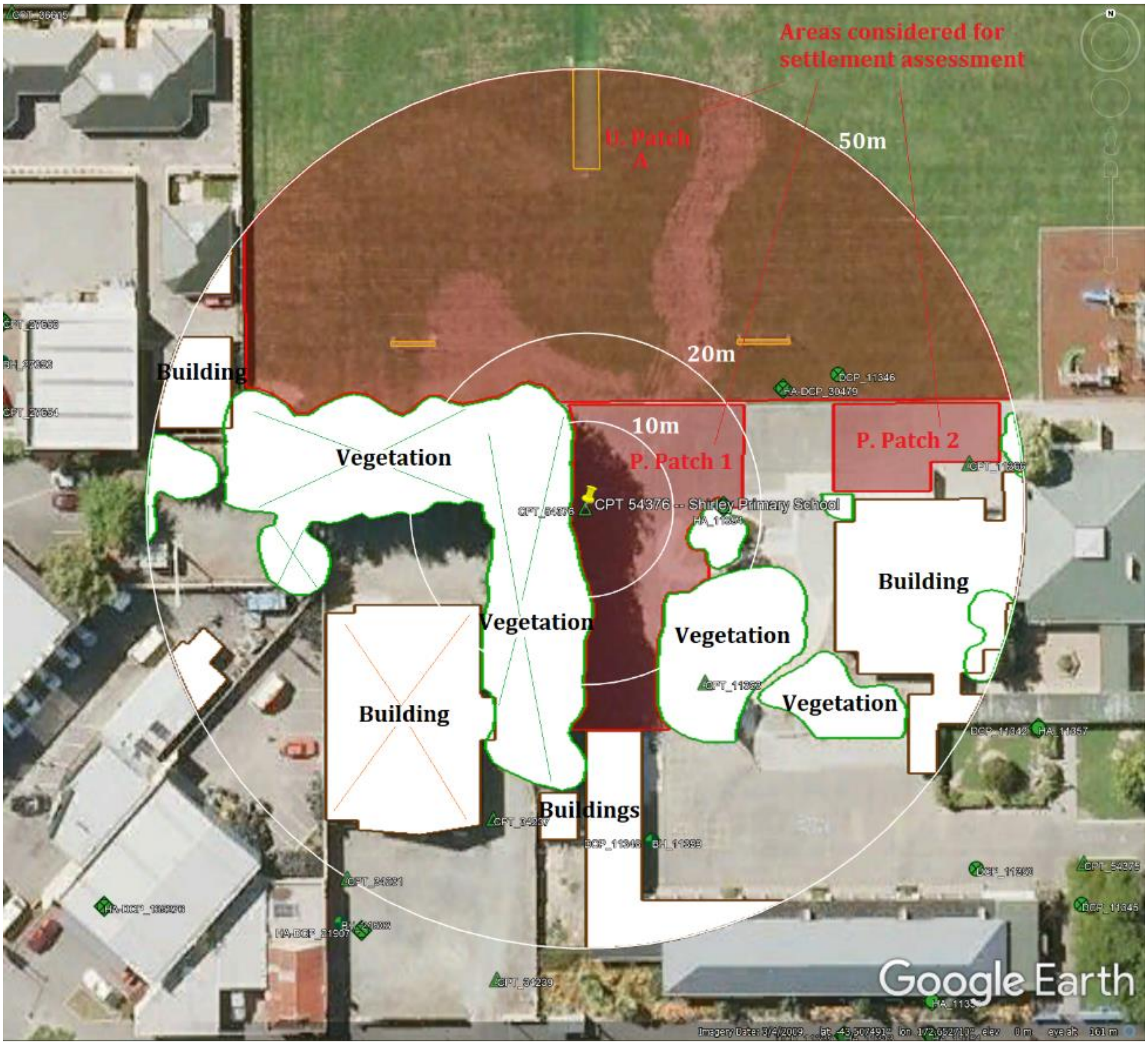

Figure 1: Site plan with areas where ejecta-induced settlement is considered.

Note 1: Three patches (outlined in red) in the free field were selected for settlement assessment as areas free of vegetation and structures. Other important factors considered for the patch selection were the proximity of a patch to a CPT, a property subjected to addition and/or demolition of a structure, and front yard/backyard alterations (e.g., ploughing, rubble, scrap), and aerial distribution of sediment ejecta. Paved Patch 2 is the only portion of the site that was analyzed for the ejecta-induced settlement using the LiDAR data because the anthropogenic changes between the LiDAR surveys affected the rest of the site. The LiDAR-based settlement analyses of Paved Patch 2 were not performed for the Sep-10 and Dec-11 EQs due to the evident absence of ejecta.

Table 2: LiDAR flight error adjustments, global adjustments for the difference between average LiDAR point elevations and benchmark survey elevations, and vertical tectonic movement adjustments.

	Adjustments (mm)		
Earthquake Event(s)	LiDAR Flight Error	Global Offset[2]	Tectonic Vertical Movement
Sep-10	-100	-3	0
Feb-11	+100	16	-80
Jun-11	0	38	-35
Dec-11	-50	-65	0
CES	-50	-14	-115
Any LiDAR survey affected by ejecta?			No

Note: The negative sign indicates the subtraction from the ground surface subsidence, while the positive sign indicates the addition to the ground surface subsidence.

Table 3: LiDAR Measurement Error for P. Patch 2.

Surveys	Buffer	Area Averaged Difference Indicating Repeat Measurement Error (mm)	ϭ*$_{individual}$ LiDAR points (mm)	%Reduction in ϭ due to Area Averaging of LiDAR Points
Post Feb 2011: Mar 2011 and May 2011	10-m	NA	59	[7,7]
	20-m	NA		
	50-m	4		
Post Dec 2011: Feb 2012 and Oct 2015	10-m	NA	70	[ND,ND]
	20-m	NA		
	50-m	ND		

*Standard deviation; NA = Not available; ND = Not determined.

[2] Russell, J., & van Ballegooy, S. (2015). *Canterbury Earthquake Sequence: Increased liquefaction vulnerability assessment methodology*. New Zealand: Tonkin & Taylor Ltd.

Table 4: Ground surface subsidence adjustments due to LiDAR measurement error for P. Patch 2.

Earthquake Event(s)	$б_{pre\text{-}EQ\ LiDAR\ survey}$ (mm)	$б_{post\text{-}EQ\ LiDAR\ survey}$ (mm)	$б_{total}$ (mm)	Area Average Adjusted б (mm) **
Sep-10	158	56	134	±9
Feb-11	56	59	59	±4
Jun-11	59	61	62	±4
Dec-11	61	70	87	±6
CES	158	70	124	±8

**Based on the highest %Reduction in Table 3.

Table 5: Raw liquefaction-related ground surface subsidence using original LiDAR points for P. Patch 2.

	Average Ground Surface Subsidence (mm)		
Earthquake Event(s)	10-m Buffer	20-m Buffer	50-m Buffer
Sep-10	NA	NA	ND
Feb-11	NA	NA	180
Jun-11	NA	NA	39
Dec-11	NA	NA	ND
CES	NA	NA	ND

ND = Not determined; NA = Not available; ND = Not determined.

Table 6: Corrected liquefaction-related ground surface subsidence using original LiDAR points for P. Patch 2 with the calculated adjustments in Table 2.

	Average Calculated Ground Surface Subsidence (mm)		
Earthquake Event(s)	10-m Buffer	20-m Buffer	50-m Buffer
Sep-10	NA	NA	ND
Feb-11	NA	NA	216±25
Jun-11	NA	NA	42±25
Dec-11	NA	NA	ND
CES	NA	NA	ND

Notes: Plus/minus values are same as those in Table 4a, but rounded to the nearest 25 mm; Positive overall values indicate ground surface subsidence, while negative overall values indicate ground surface uplift; ND = Not determined; NA = Not available..

Table 7: Corrected liquefaction-related ground surface subsidence for P. Patch 2 using LiDAR DEMs.

	Estimated Ground Surface Subsidence (mm)								
	10-m Buffer			20-m Buffer			50-m Buffer		
Earthquake Event(s)	16th %ile	50th %ile	84th %ile	16th %ile	50th %ile	84th %ile	16th %ile	50th %ile	84th %ile
Sep-10	NA	NA	NA	NA	NA	NA	<50	<50	<50
Feb-11	NA	NA	NA	NA	NA	NA	150	200	250
Jun-11	NA	NA	NA	NA	NA	NA	<50	<50	50
Dec-11	NA	NA	NA	NA	NA	NA	<50	<50	100
CES	NA	NA	NA	NA	NA	NA	200	250	400

Note: These percentiles are not the exact statistical measures; they indicate the spatial variability of ground surface subsidence.

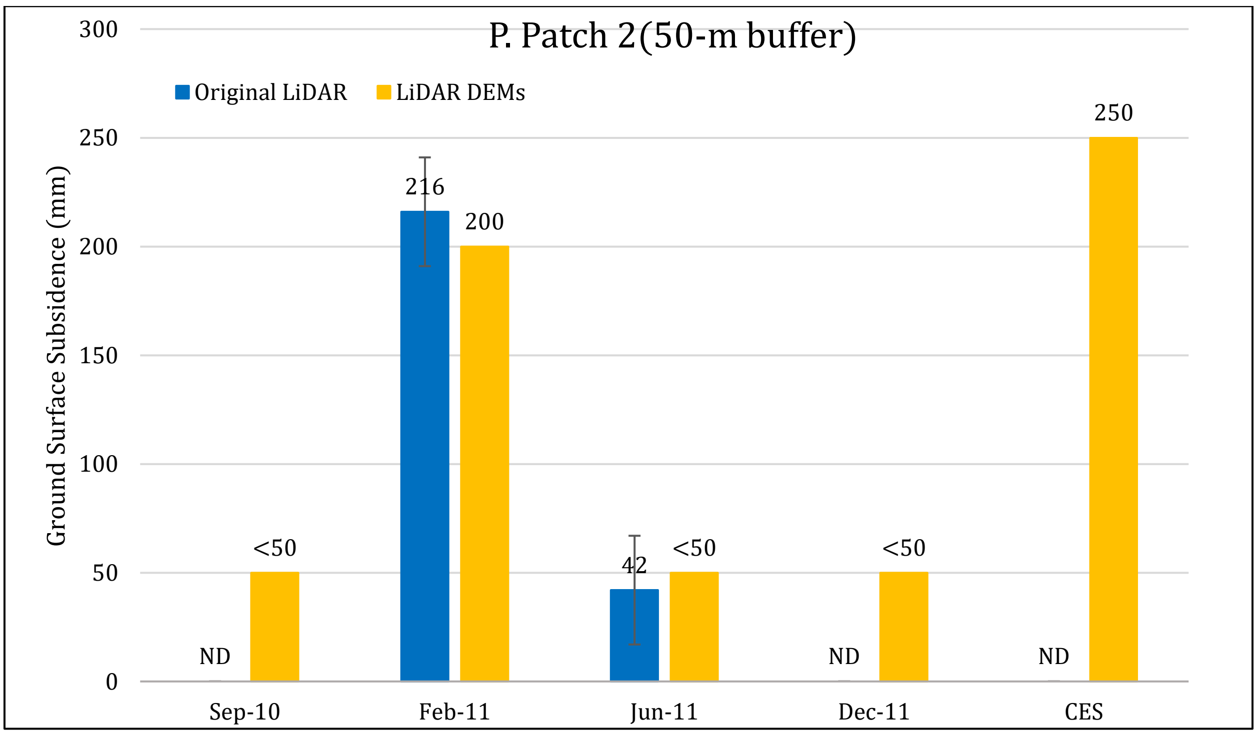

Figure 2: Comparison between ground surface subsidence determined from original LiDAR survey points and ground surface subsidence (50th %ile) estimated using LiDAR DEMs for P. Patch 2 (50-m buffer).

Note 2: The ground surface subsidence values determined using the original LiDAR survey points are similar to the ground surface subsidence values estimated using the LiDAR DEMs for all earthquake events.

Table 8a: Ejecta-Induced settlement for the top 20 m of the soil profile for P. Patch 1 (10-m buffer) for the 50th %ile PGA, P_L=50%, and C_{FC}=0.13 using BI-2014, ZRB-2002, and I_C cutoff of 2.6.

Earthquake Event(s)	M_W	PGA (g)	Depth to Groundwater (m)	S_T (mm)	S_{V1D} (mm)	$S_{E,L}$ (mm)
Sep-10	7.1	0.20	2.0	ND	12±20	ND
Feb-11	6.2	0.36	2.0	ND	69±50	ND
Jun-11	6.2	0.21	1.5	ND	11±25	ND
Dec-11	6.1	0.25	1.5	ND	23±50	ND

Notes: S_T = Total settlement (Table 6); S_{V1D} = Average vertical settlement due to volumetric compression using Boulanger and Idriss (2014) (BI-2014), Zhang et al. (2002) (ZRB-2002) procedures and de Greef and Lengkeek (2018) thin-layer correction; $S_{E,L}$ = Ejecta-induced settlement as the difference between the LiDAR-based S_T and S_{V1D}.

Table 8b: Ejecta-Induced settlement for the top 20 m of the soil profile for P. Patch 1 (20-m buffer) for the 50th %ile PGA, P_L=50%, and C_{FC}=0.13 using BI-2014, ZRB-2002, and I_C cutoff of 2.6.

Earthquake Event(s)	M_W	PGA (g)	Depth to Groundwater (m)	S_T (mm)	S_{V1D} (mm)	$S_{E,L}$ (mm)
Sep-10	7.1	0.20	2.0	ND	23±20	ND
Feb-11	6.2	0.36	2.0	ND	98±50	ND
Jun-11	6.2	0.21	1.5	ND	23±25	ND
Dec-11	6.1	0.25	1.5	ND	41±50	ND

Notes: S_T = Total settlement (Table 6); S_{V1D} = Average vertical settlement due to volumetric compression using Boulanger and Idriss (2014) (BI-2014), Zhang et al. (2002) (ZRB-2002) procedures and de Greef and Lengkeek (2018) thin-layer correction; $S_{E,L}$ = Ejecta-induced settlement as the difference between the LiDAR-based S_T and S_{V1D}.

Table 8c: Ejecta-Induced settlement for the top 20 m of the soil profile for P. Patch 1 (50-m buffer) for the 50th %ile PGA, P_L=50%, and C_{FC}=0.13 using BI-2014, ZRB-2002, and I_C cutoff of 2.6.

Earthquake Event(s)	M_W	PGA (g)	Depth to Groundwater (m)	S_T (mm)	S_{V1D} (mm)	$S_{E,L}$ (mm)
Sep-10	7.1	0.20	2.0	ND	36±20	ND
Feb-11	6.2	0.36	2.0	ND	127±50	ND
Jun-11	6.2	0.21	1.5	ND	32±25	ND
Dec-11	6.1	0.25	1.5	ND	57±50	ND

Notes: S_T = Total settlement (Table 6); S_{V1D} = Average vertical settlement due to volumetric compression using Boulanger and Idriss (2014) (BI-2014), Zhang et al. (2002) (ZRB-2002) procedures and de Greef and Lengkeek (2018) thin-layer correction; $S_{E,L}$ = Ejecta-induced settlement as the difference between the LiDAR-based S_T and S_{V1D}.

Table 8d: Ejecta-Induced settlement for the top 20 m of the soil profile for P. Patch 2 for the 50th %ile PGA, P_L=50%, and C_{FC}=0.13 using BI-2014, ZRB-2002, and I_C cutoff of 2.6.

Earthquake Event(s)	M_W	PGA (g)	Depth to Groundwater (m)	S_T (mm)	S_{V1D} (mm)	$S_{E,L}$ (mm)
Sep-10	7.1	0.20	2.0	ND	6±20	ND
Feb-11	6.2	0.36	2.0	216±25	35±50	181±56
Jun-11	6.2	0.21	1.5	42±25	5±25	37±35
Dec-11	6.1	0.25	1.5	ND	10±50	ND

Notes: S_T = Total settlement (Table 6); S_{V1D} = Average vertical settlement due to volumetric compression using Boulanger and Idriss (2014) (BI-2014), Zhang et al. (2002) (ZRB-2002) procedures and de Greef and Lengkeek (2018) thin-layer correction; $S_{E,L}$ = Ejecta-induced settlement as the difference between the LiDAR-based S_T and S_{V1D}.

Table 8e: Ejecta-Induced settlement for the top 20 m of the soil profile for Patch A for the 50th %ile PGA, P_L=50%, and C_{FC}=0.13 using BI-2014, ZRB-2002, and I_C cutoff of 2.6.

Earthquake Event(s)	M_W	PGA (g)	Depth to Groundwater (m)	S_T (mm)	S_{V1D} (mm)	$S_{E,L}$ (mm)
Sep-10	7.1	0.20	2.0	ND	37±20	ND
Feb-11	6.2	0.36	2.0	ND	99±50	ND
Jun-11	6.2	0.21	1.5	ND	32±25	ND
Dec-11	6.1	0.25	1.5	ND	49±50	ND

Notes: S_T = Total settlement (Table 6); S_{V1D} = Average vertical settlement due to volumetric compression using Boulanger and Idriss (2014) (BI-2014), Zhang et al. (2002) (ZRB-2002) procedures and de Greef and Lengkeek (2018) thin-layer correction; $S_{E,L}$ = Ejecta-induced settlement as the difference between the LiDAR-based S_T and S_{V1D}.

Note 3: The uncertainty for volumetric settlement was derived based on the sensitivity of volumetric settlement to PGA, C_{FC}, and P_L for each earthquake event for VsVp 57203 *Shirley Intermediate School* and CC LIQ 1 – CPT 5586 – *Vivian St* sites. Taking the 50th percentile as the baseline case, the minimum and maximum values corresponding to the difference between the 25th percentile and the 50th percentile and the 75th percentile and the 50th percentile were determined. The arithmetic mean of the range of the minimum and maximum difference was evaluated for each patch at the two sites. The maximum arithmetic mean for each earthquake event was rounded to the nearest five and used as the uncertainty value. Accordingly, the 1-D volumetric settlement uncertainties of ±20, ±50, ±25, and ±50 mm for the Sep-10, Feb-11, Jun-11, and Dec-11 earthquake events, respectively, were used for all sites in this study.

Table 9a: Coverage area and height of ejecta estimates for P. Patch 1 (10-m buffer) using photographs.

Earthquake Event	$H_{E,thick1}$ (mm)	$A_{E,thick1}$ (m²)	$H_{E,thick2}$ (mm)	$A_{E,thick2}$ (m²)	$H_{E,thin}$ (mm)	$A_{E,thin}$ (m²)	A_T (m²)
Sep-10	0	0	0	0	0	0	117
Feb-11	80-160	41.3	40-60	46.3	10-20	29.4	117
Jun-11	40-80	19.0	30-50	15.4	10-20	26.9	153
Dec-11	0	0	0	0	0	0	117

Notes: $A_{E,thick/thin}$ = Coverage area of thick/thin ejecta layers; $H_{E,thick/thin}$ = Lower-upper estimate of height of thick/thin ejecta layers; Thin and thick layers correspond to light gray and dark gray colors of ejecta observed in aerial photographs; A_T = Total assessment area of a buffer being considered.

Table 9b: Coverage area and height of ejecta estimates for P. Patch 1 (20-m buffer) using photographs.

Earthquake Event	$H_{E,thick1}$ (mm)	$A_{E,thick1}$ (m²)	$H_{E,thick2}$ (mm)	$A_{E,thick2}$ (m²)	$H_{E,thin}$ (mm)	$A_{E,thin}$ (m²)	A_T (m²)
Sep-10	0	0	0	0	0	0	348
Feb-11	80-160	152	40-60	113	10-20	82.9	348
Jun-11	40-80	89.1	30-50	49.7	10-20	79.8	357
Dec-11	0	0	0	0	0	0	348

Notes: $A_{E,thick/thin}$ = Coverage area of thick/thin ejecta layers; $H_{E,thick/thin}$ = Lower-upper estimate of height of thick/thin ejecta layers; Thin and thick layers correspond to light gray and dark gray colors of ejecta observed in aerial photographs; A_T = Total assessment area of a buffer being considered.

Table 9c: Coverage area and height of ejecta estimates for P. Patch 1 (50-m buffer) using photographs.

Earthquake Event	$H_{E,thick1}$ (mm)	$A_{E,thick1}$ (m²)	$H_{E,thick2}$ (mm)	$A_{E,thick2}$ (m²)	$H_{E,thin}$ (mm)	$A_{E,thin}$ (m²)	A_T (m²)
Sep-10	0	0	0	0	0	0	391
Feb-11	80-160	181	40-60	116	10-20	94.0	391
Jun-11	40-80	90.2	30-50	74.3	10-20	79.8	391
Dec-11	0	0	0	0	0	0	391

Notes: $A_{E,thick/thin}$ = Coverage area of thick/thin ejecta layers; $H_{E,thick/thin}$ = Lower-upper estimate of height of thick/thin ejecta layers; Thin and thick layers correspond to light gray and dark gray colors of ejecta observed in aerial photographs; A_T = Total assessment area of a buffer being considered.

Table 9d: Coverage area and height of ejecta estimates for Patch A (50-m buffer) using photographs.

EQ Event	$A_{E,thick1}$ (m²)	$H_{E,thick1}$ (m)	$A_{E,thick2}$ (m²)	$H_{E,thick2}$ (m)	$A_{E,thin1}$ (m²)	$H_{E,thin1}$ (m)	$A_{E,thin2}$ (m²)	$H_{E,thin2}$ (m)	A_T (m²)
Sep-10	0	0	0	0	0	0	0	0	2519
Feb-11	717	200-300	54.3	80-160	248	60-80	251	5-10	2519
Jun-11	0	0	259	60-100	87.4	30-60	399	10-20	2531
Dec-11	0	0	0	0	0	0	0	0	2519

Notes: $A_{E,thin/thick}$ = Coverage area of thin/thick ejecta layers; $H_{E,thin/thick}$ = Lower-upper estimate of height of thin ejecta layers; A_T= Total assessment area of a buffer being considered.

Table 9e: Coverage area and height of ejecta estimates for P. Patch 2 (50-m buffer) using photographs.

Earthquake Event	$A_{E,thick}$ (m²)	$H_{E,thick}$ (m)	$A_{E,thin}$ (m²)	$H_{E,thin}$ (m)	A_T (m²)
Sep-10	0	0	0	0	166
Feb-11	71.5	40-60	94.5	5-15	166
Jun-11	8.5	20-40	31.5	5-15	166
Dec-11	0	0	0	0	166

Notes: $A_{E,thick/thin}$ =Coverage area of thick/thin ejecta layers; $H_{E,thick/thin}$ = Lower-upper estimate of height of thick/thin ejecta layers; A_T= Total assessment area of a buffer being considered; Thin and thick layers correspond to light gray and dark gray colors of ejecta observed in aerial photographs.

Note 4: The values in Table 9 correspond to the coverage area of ejecta outlined in aerial photographs (Figures 10, 11, 26, 29, 30, 54, and 55) and the lower and upper estimates of ejecta height based on geometrical approximations, ground photographs (Figure 56), and EQC LDAT property inspection reports. The ejecta-induced settlement using photographs and engineering judgment, $S_{E,P}$, is estimated as

$$S_{E,P} = \frac{\sum_{i=1}^{a} A_{E,thick,i} * H_{E,thick,i} + \sum_{j=1}^{b} A_{E,thin,j} * H_{E,thin,j}}{A_T} = \frac{\sum_{i=1}^{a} V_{E,thick,i} + \sum_{j=1}^{b} V_{E,thin,j}}{A_T}$$

where

- $A_{E,thick,i}$ and $H_{E,thick,i}$ are the area and the height of a thick ejecta layer, respectively;
- $A_{E,thin,j}$ and $H_{E,thin,j}$ are the area and the height of a thin ejecta layer, respectively;
- A_T is the total assessment area for a buffer being considered (Figure 1).

Table 10a: Ejecta-induced settlement estimates for P. Patch 1 based on photographs.

Earthquake Event	P. Patch 1 (10-m buffer)		P. Patch 1 (20-m buffer)		P. Patch 1 (50-m buffer)	
	$S_{E,P,lower}$ (mm)	$S_{E,P,upper}$ (mm)	$S_{E,P,lower}$ (mm)	$S_{E,P,upper}$ (mm)	$S_{E,P,lower}$ (mm)	$S_{E,P,upper}$ (mm)
Sep-10	0	0	0	0	0	0
Feb-11	47	85	50	94	51	97
Jun-11	10	19	16	31	17	32
Dec-11	0	0	0	0	0	0

Note: $S_{E,P,lower}$ and $S_{E,P,upper}$ correspond to lower and upper estimates of $S_{E,P}$, respectively.

Table 10b: Ejecta-induced settlement estimates for Patch A and P. Patch 2 based on photographs.

Earthquake Event	Patch A (50-m buffer)		P. Patch 2 (50-m buffer)	
	$S_{E,P,lower}$ (mm)	$S_{E,P,upper}$ (mm)	$S_{E,P,lower}$ (mm)	$S_{E,P,upper}$ (mm)
Sep-10	0	0	0	0
Feb-11	65	98	20	34
Jun-11	9	16	2	5
Dec-11	0	0	0	0

Note: $S_{E,P,lower}$ and $S_{E,P,upper}$ correspond to lower and upper estimates of $S_{E,P}$, respectively.

Table 11a: Best final estimates of ejecta-induced settlement for P. Patch 1.

EQ Event	P. Patch 1 (10-m buffer)			P. Patch 1 (20-m buffer)			P. Patch 1 (50-m buffer)		
	$S_{E,L}$ (mm)	$S_{E,P}$ (mm)	$S_{E,final}$ (mm)	$S_{E,L}$ (mm)	$S_{E,P}$ (mm)	$S_{E,final}$ (mm)	$S_{E,L}$ (mm)	$S_{E,P}$ (mm)	$S_{E,final}$ (mm)
Sep-10	ND	0	0	ND	0	0	ND	0	0
Feb-11	ND	66±19	65±20	ND	72±22	70±20	ND	74±23	75±25
Jun-11	ND	15±4	15±5	ND	24±7	25±5	ND	25±7	25±5
Dec-11	ND	0	0	ND	0	0	ND	0	0

Notes: $S_{E,L}$ = Ejecta-induced settlement based on LiDAR data reported in Table 8; $S_{E,P}$ = Median ejecta-induced settlement for the range of values reported in Table 10; $S_{E,final}$ = Best final estimate of ejecta-induced settlement rounded to the nearest 5 mm; Final plus/minus values are also rounded to the nearest 5 mm; ND= Not determined.

Table 11b: Best final estimates of ejecta-induced settlement for Patch A and P. Patch 2 based on photographs.

Earthquake Event	Patch A (50-m buffer)			P. Patch 2 (50-m buffer)		
	$S_{E,L}$ (mm)	$S_{E,P}$ (mm)	$S_{E,final}$ (mm)	$S_{E,L}$ (mm)	$S_{E,P}$ (mm)	$S_{E,final}$ (mm)
Sep-10	ND	0	0	ND	0	0
Feb-11	ND	82±16	80±15	181±56	27±7	40±10
Jun-11	ND	12.5±3.5	15±5	37±35	3.5±1.5	5±5
Dec-11	ND	0	0	ND	0	0

Notes: $S_{E,L}$ = Ejecta-induced settlement based on LiDAR data reported in Table 8; $S_{E,P}$ = Median ejecta-induced settlement for the range of values reported in Table 10; $S_{E,final}$ = Best final estimate of ejecta-induced settlement rounded to the nearest 5; Final plus/minus values are also rounded to the nearest 5; ND= Not determined.

Note 5:

- P. Patch 1 and Patch A: $S_{E,final}$ is based solely on $S_{E,P}$ for all earthquake events due to the anthropogenic changes affecting the LiDAR survey measurements.
- P. Patch 2: $S_{E,final}$ for the Sep-10 and Dec-11 EQs is equal to $S_{E,P}$ due to the evident absence of ejecta. $S_{E,final}$ for the Feb-11 and Jun-11 EQs is a weighted average of $S_{E,L}$ and $S_{E,P}$ with weights of 0.1 and 0.9, respectively. The uncertainty associated with $S_{E,final}$ is also a weighted average of uncertainties associated with $S_{E,L}$ and $S_{E,P}$ with the same weights of 0.1 and 0.9, respectively.
- The weight coefficients are based on the LiDAR error bands, LPI prediction error (Maurer et al. 2014[3]), presence of ejecta at the time of LiDAR surveys, and completeness of visual evidence (i.e., ground and aerial photographs and EQC LDAT property inspection reports for the site). The Shirley Primary School site is in the apparent zone of higher ground surface subsidence for the Sep-10 EQ and the apparent zone of lower ground surface subsidence (i.e., the underestimate of the ground surface elevation by the Sep-10 LiDAR survey). The site is also in the zone of slight LPI overprediction of liquefaction severity for the Sep-10 EQ and slight to moderate LPI underprediction of liquefaction severity for the Feb-11 EQ. The LDAT property inspection reports are available for nearby properties, where the maximum ejecta height was recorded as 300-400 mm. The ground photographs showing remnants of ejecta at the nearby properties are also available.

<u>Summary 1</u>:

- **The best estimate of the ejecta-induced free-field ground settlement of the unpaved surface at the Shirley Primary School site for the SEP 2010, FEB 2011, JUN 2011, and DEC 2011 earthquake is 0 mm, 80±15 mm, 15±5 mm, and 0 mm, respectively.**
- **The best estimate of the ejecta-induced free-field ground settlement of the paved surface at the Shirley Primary School site for the SEP 2010, FEB 2011, JUN 2011, and DEC 2011 earthquake is 0 mm, 75±25 mm, 25±5 mm, and 0 mm, respectively.**
- **The ejecta-induced settlement of the paved surface is more representative of the site.**

[3] Maurer, B. W., Green, R. A., Cubrinovski, M., & Bradley, B. A. (2014). Evaluation of the Liquefaction Potential Index for Assessing Liquefaction Hazard in Christchurch, New Zealand. *Journal of Geotechnical and Geoenvironmental Engineering*, 140(7), 04014032-1-11. doi:10.1061/(asce)gt.1943-5606.0001117

Figure 3: Location of the site.

Figure 4: Position of the site relative to nearby buildings, vegetation, and free-face features.

Figure 5: Street view of the flat land.

Figure 6: Satellite image of the site taken in Dec 2004.

Figure 7: Satellite image of the site taken in Apr 2005.

Figure 8: Satellite image of the site taken in Apr 2005.

Figure 9: Satellite image of the site taken in Mar 2009.

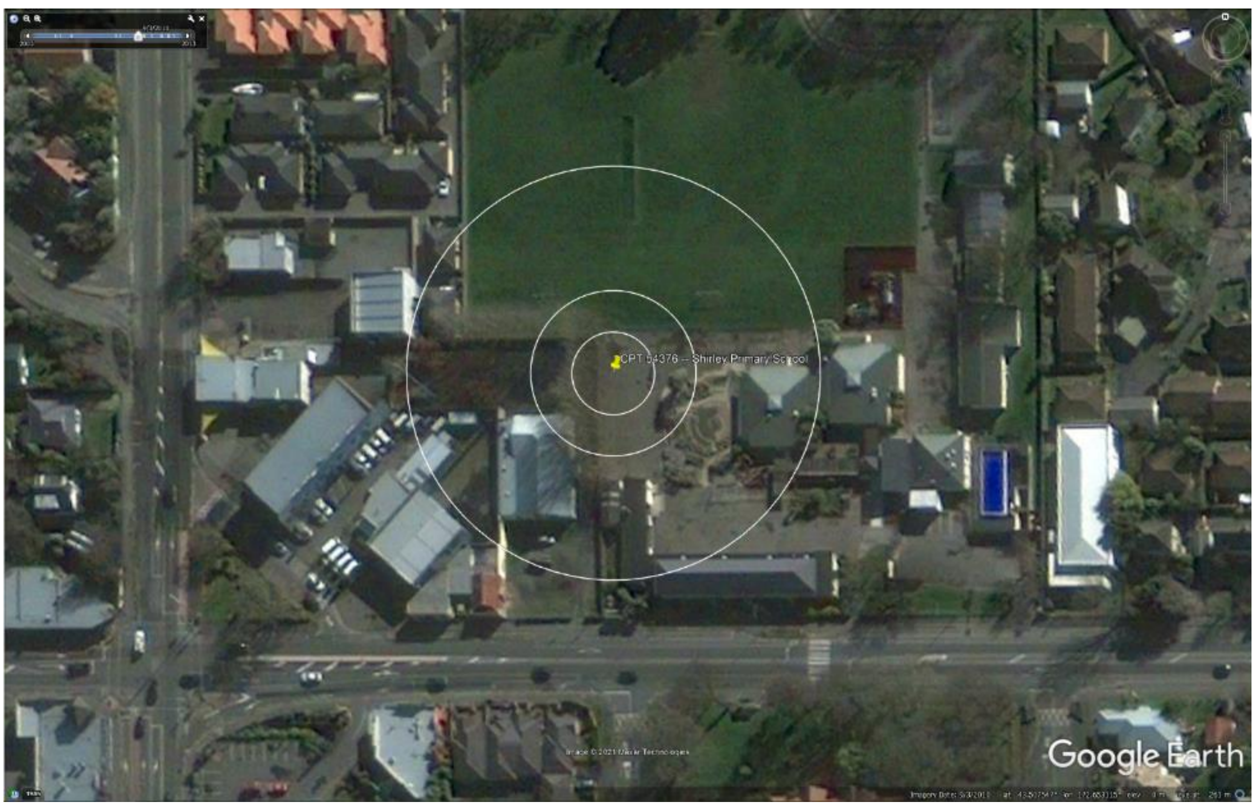

Figure 10: Satellite image of the site taken on Sep 3, 2010.

Figure 11: Satellite image of the site taken on Sep 5, 2010.

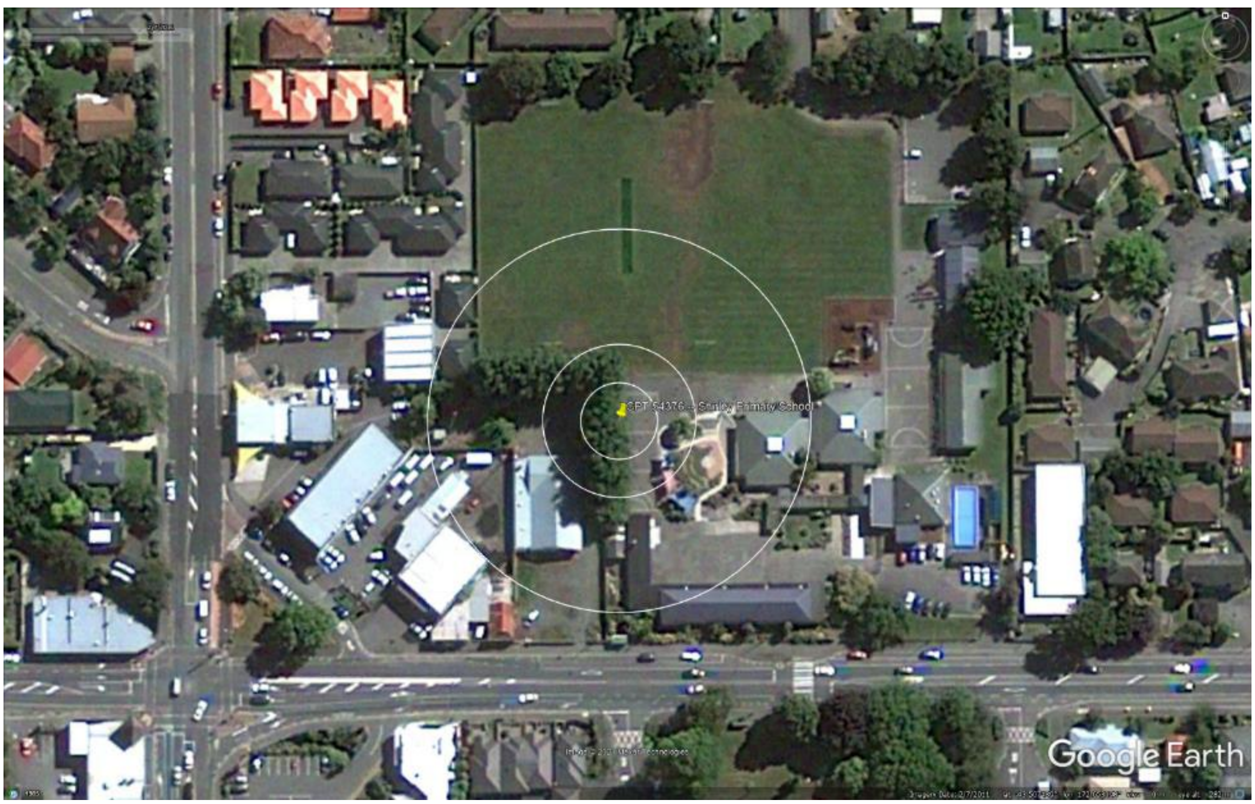

Figure 12: Satellite image of the site taken on Feb 7, 2011.

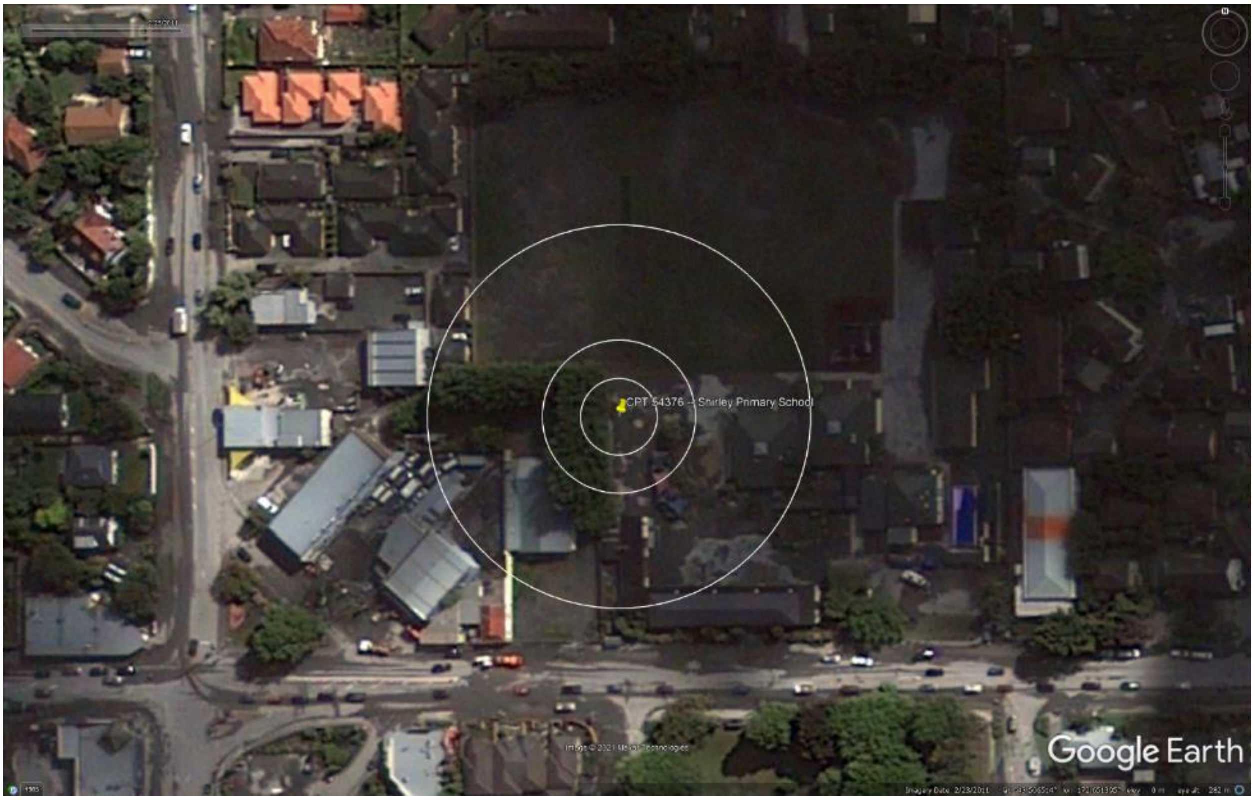

Figure 13: Satellite image of the site taken on Feb 23, 2011.

Figure 14: Satellite image of the site taken on Feb 26, 2011.

Figure 15: Satellite image of the site taken on Mar 28, 2011.

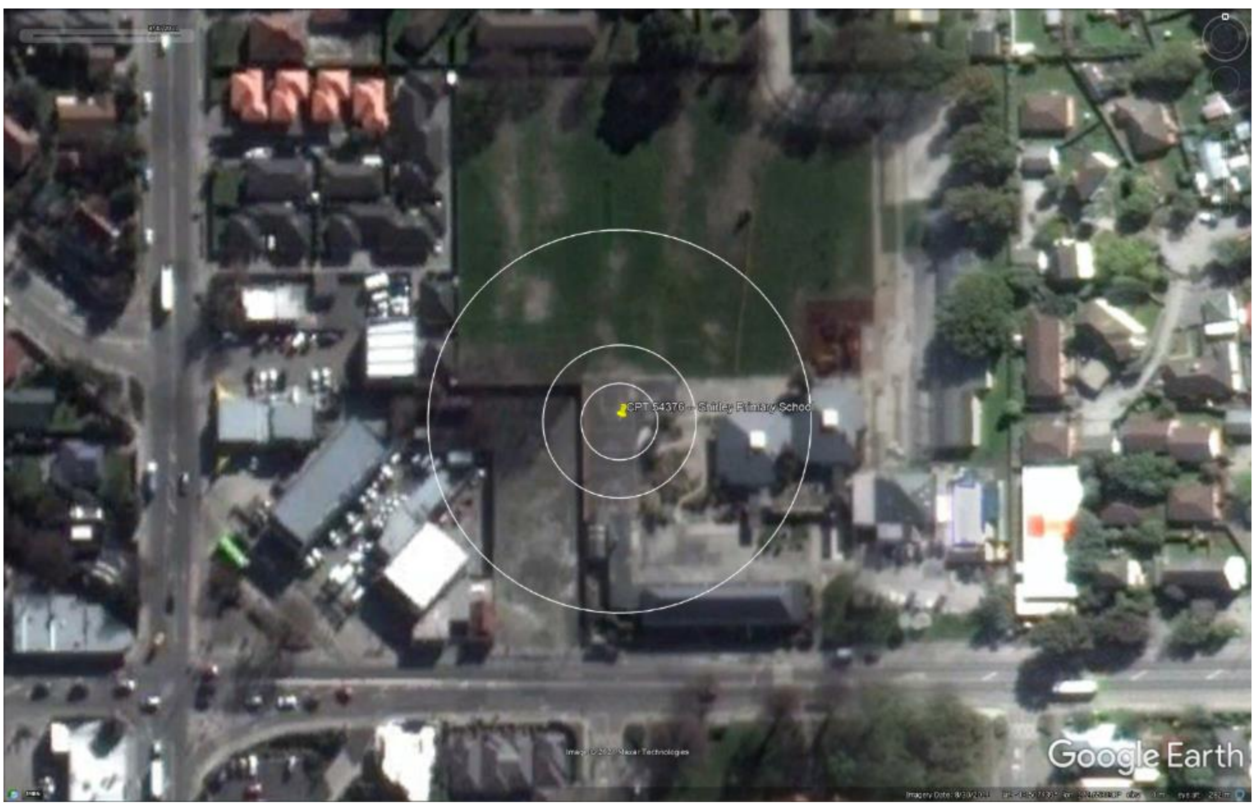

Figure 16: Satellite image of the site taken on Aug 30, 2011.

Figure 17: Satellite image of the site taken in Apr 2012.

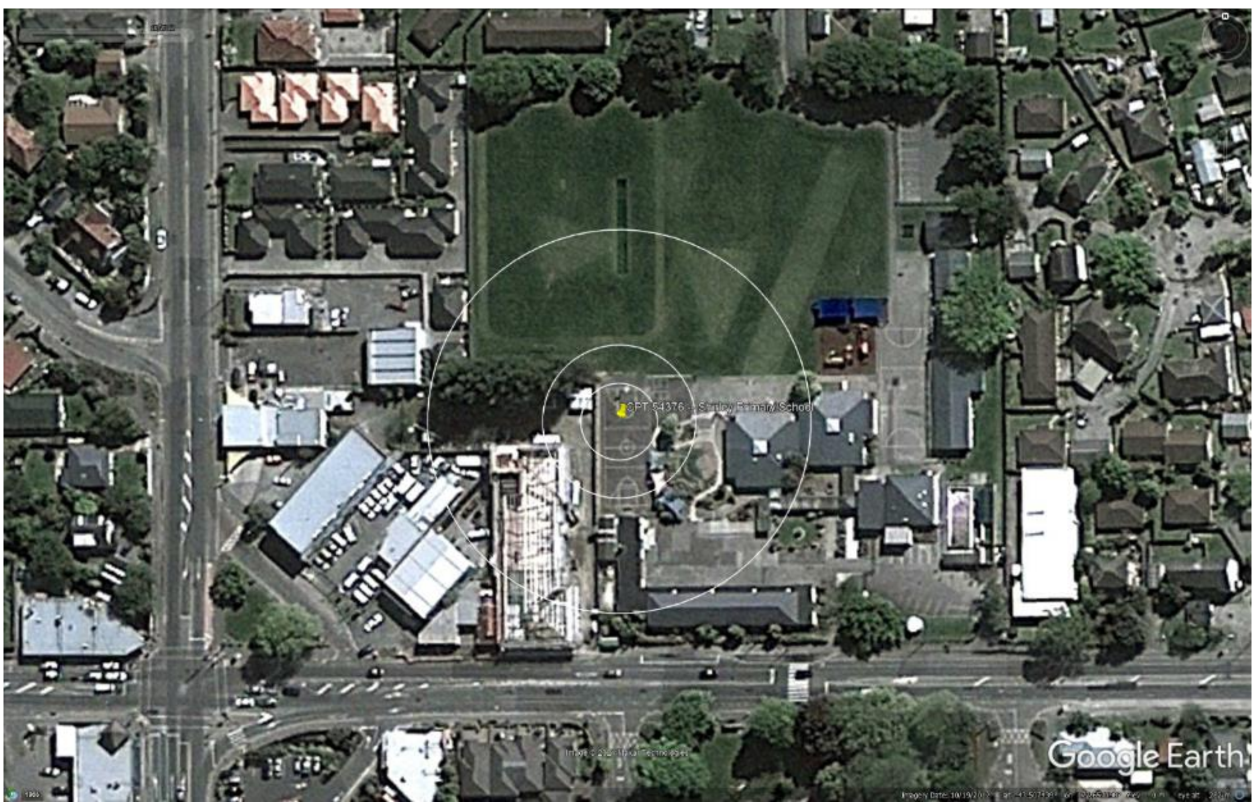

Figure 18: Satellite image of the site taken in Oct 2012.

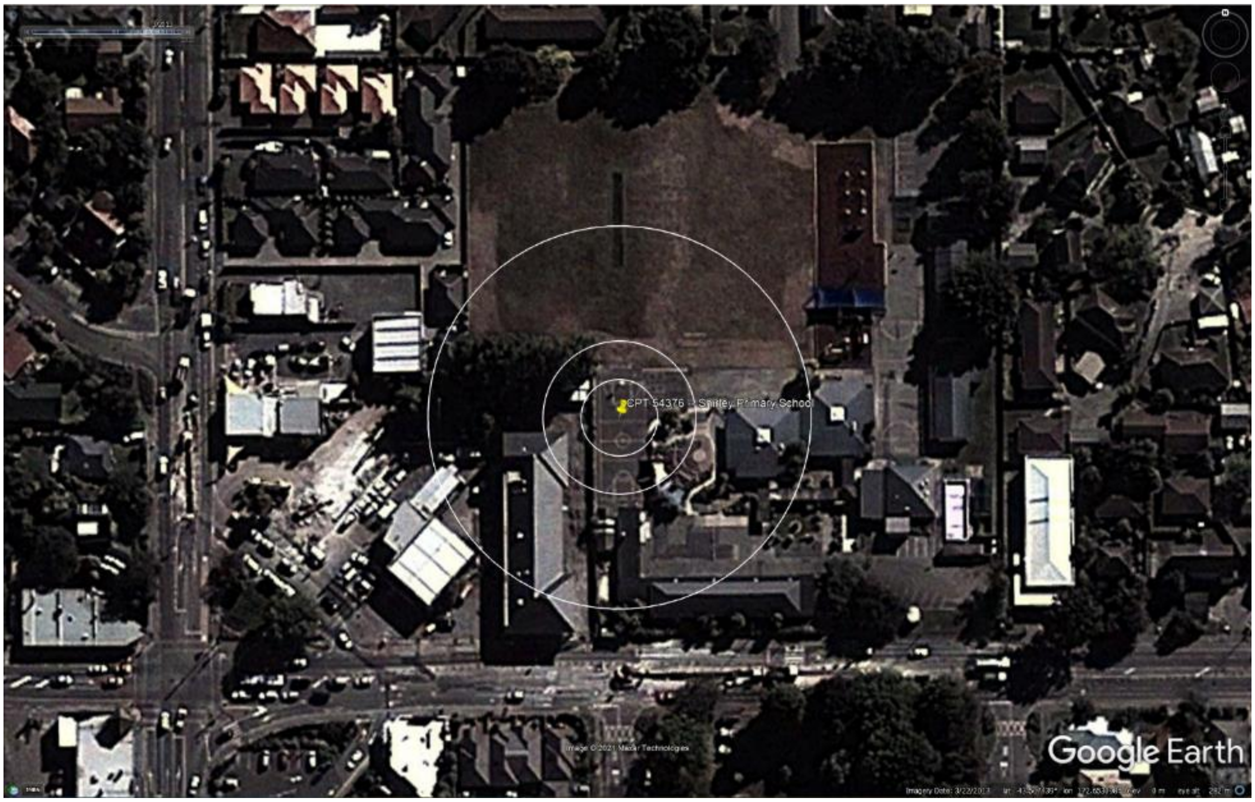

Figure 19: Satellite image of the site taken in Mar 2013.

Figure 20: Satellite image of the site taken in Aug 2013.

Figure 21: Satellite image of the site taken in Jan 2014.

Figure 22: Satellite image of the site taken in Jan 2015.

Figure 23: Satellite image of the site taken in Jun 2015.

Figure 24: Satellite image of the site taken in Sep 2015.

Figure 25: Satellite image of the site taken in Nov 2015.

Figure 26: Aerial photograph of the site taken on Sep 4, 2010.

Figure 27: Aerial photograph of the site taken on Feb 24, 2011.

Figure 28: Aerial photograph of the site taken on June 14-15, 2011.

Figure 29: Aerial photograph of the site taken on June 16, 2011.

Figure 30: Aerial photograph of the site taken on Dec 24, 2011.

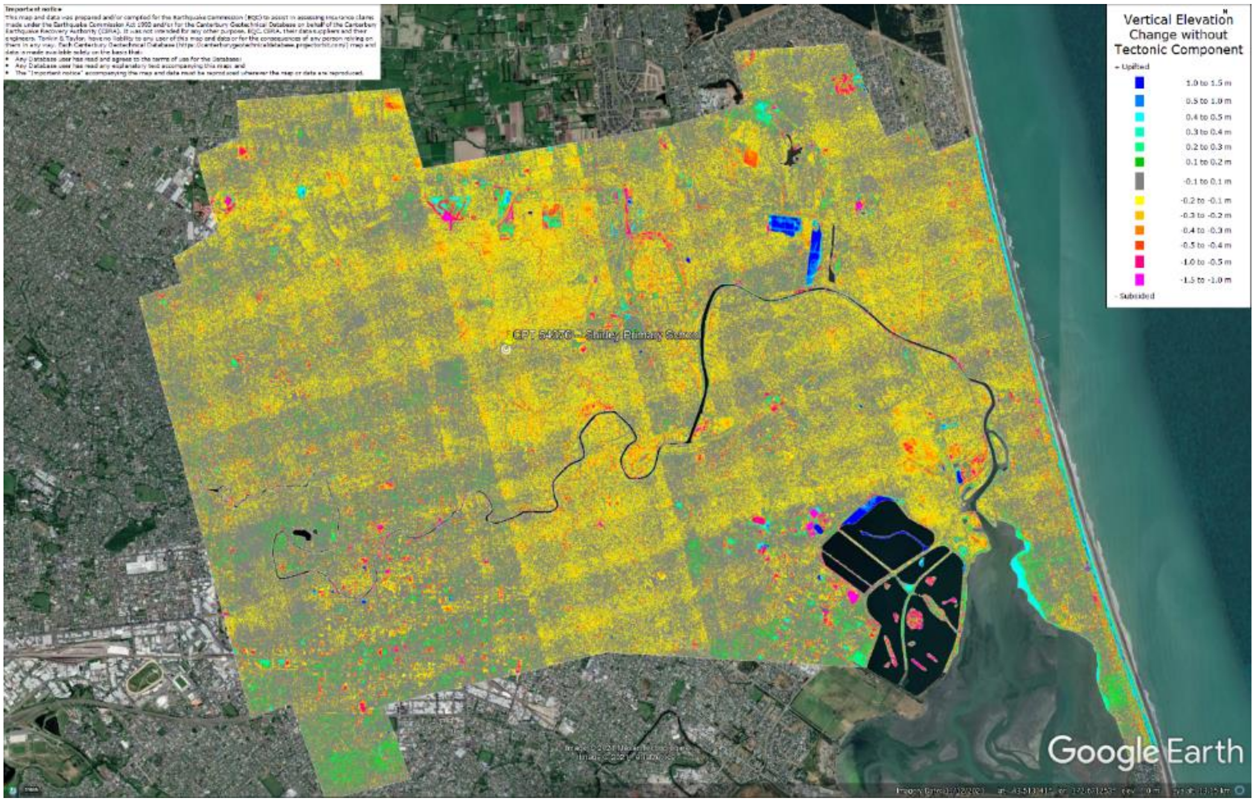

Figure 31: Vertical Ground Movements (Surface – Tectonic) for Sep 2010 Earthquake – the site is in the apparent zone of overestimated ground surface subsidence (i.e., flight error band for the Sep 2010 LiDAR survey).

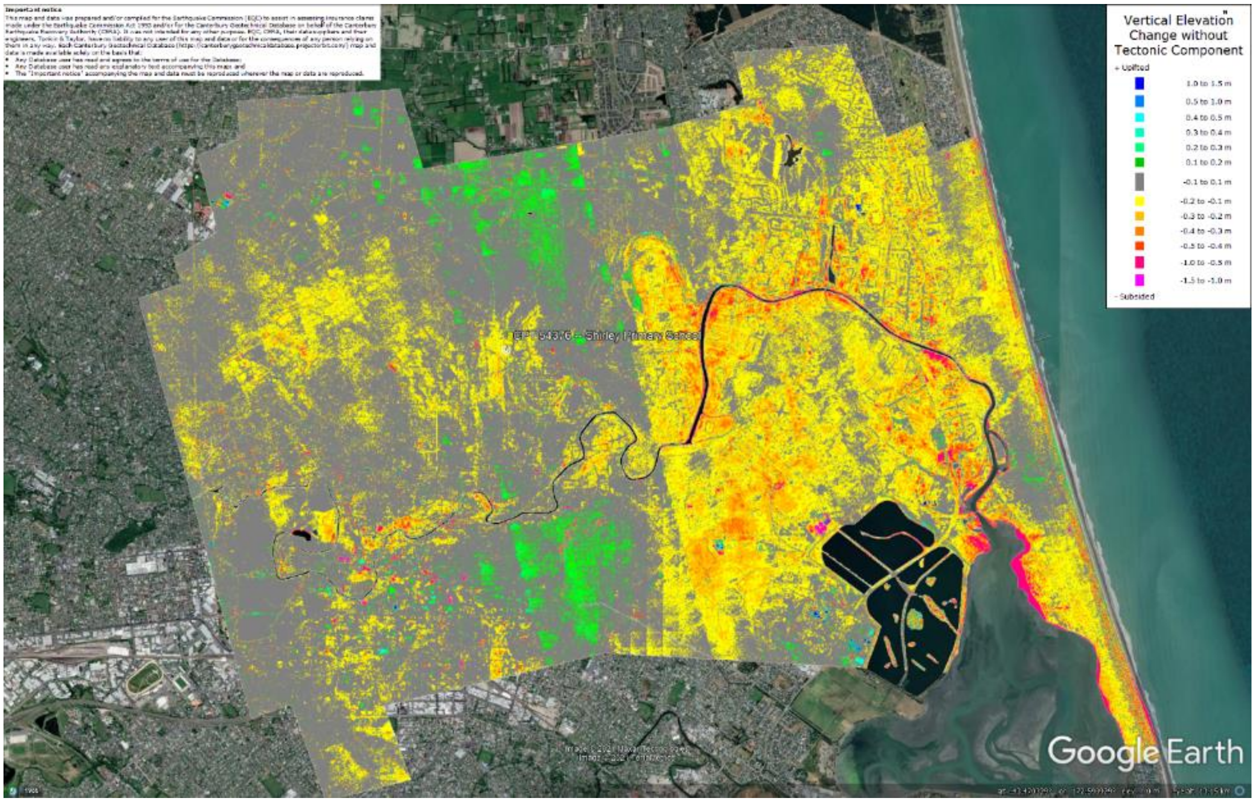

Figure 32: Vertical Ground Movements (Surface – Tectonic) for Feb 2011 Earthquake – the site is in the apparent zone of underestimated ground surface subsidence (i.e., flight error band for the Sep 2010 LiDAR survey).

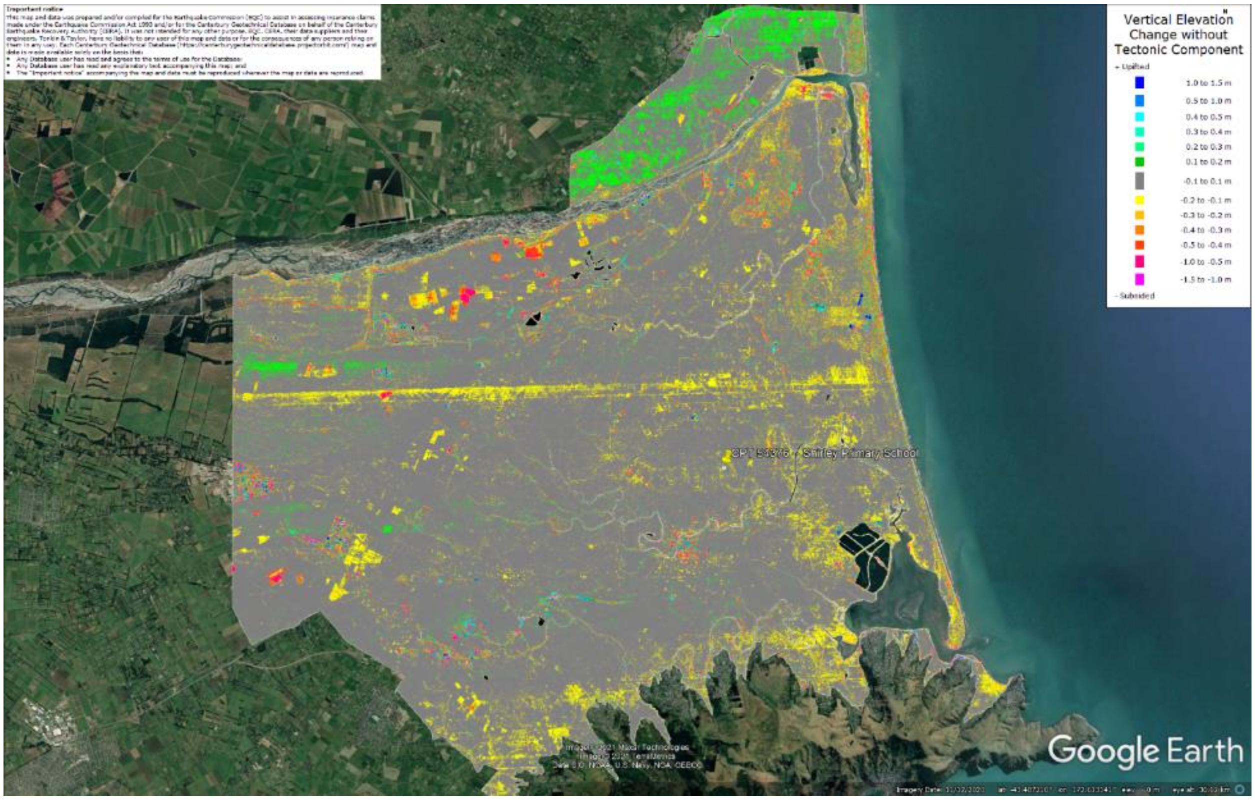

Figure 33: Vertical Ground Movements (Surface – Tectonic) for June 2011 Earthquake – the site is not in the apparent zone of overestimated/underestimated ground surface subsidence.

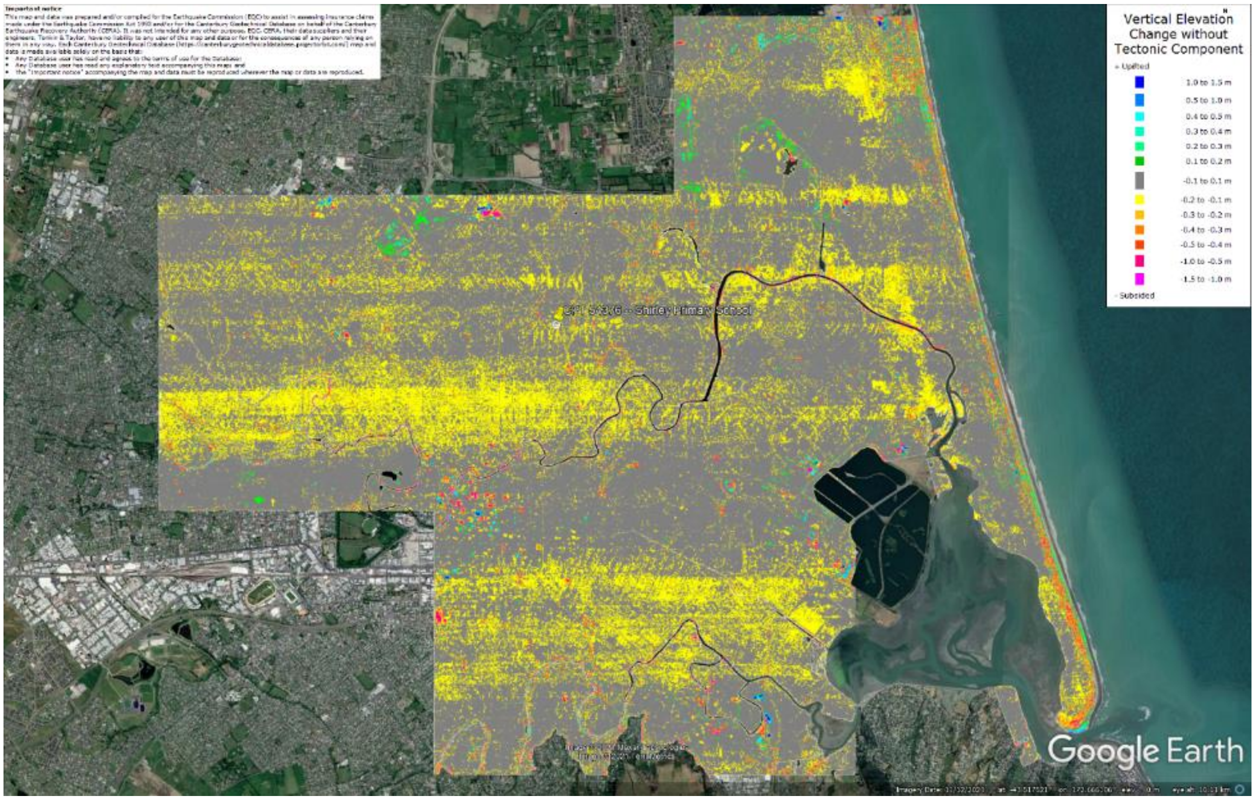

Figure 34: Vertical Ground Movements (Surface – Tectonic) for Dec 2011 Earthquake – the site is in the apparent zone of overestimated ground surface subsidence (i.e., flight error band for the Feb 2012 LiDAR survey).

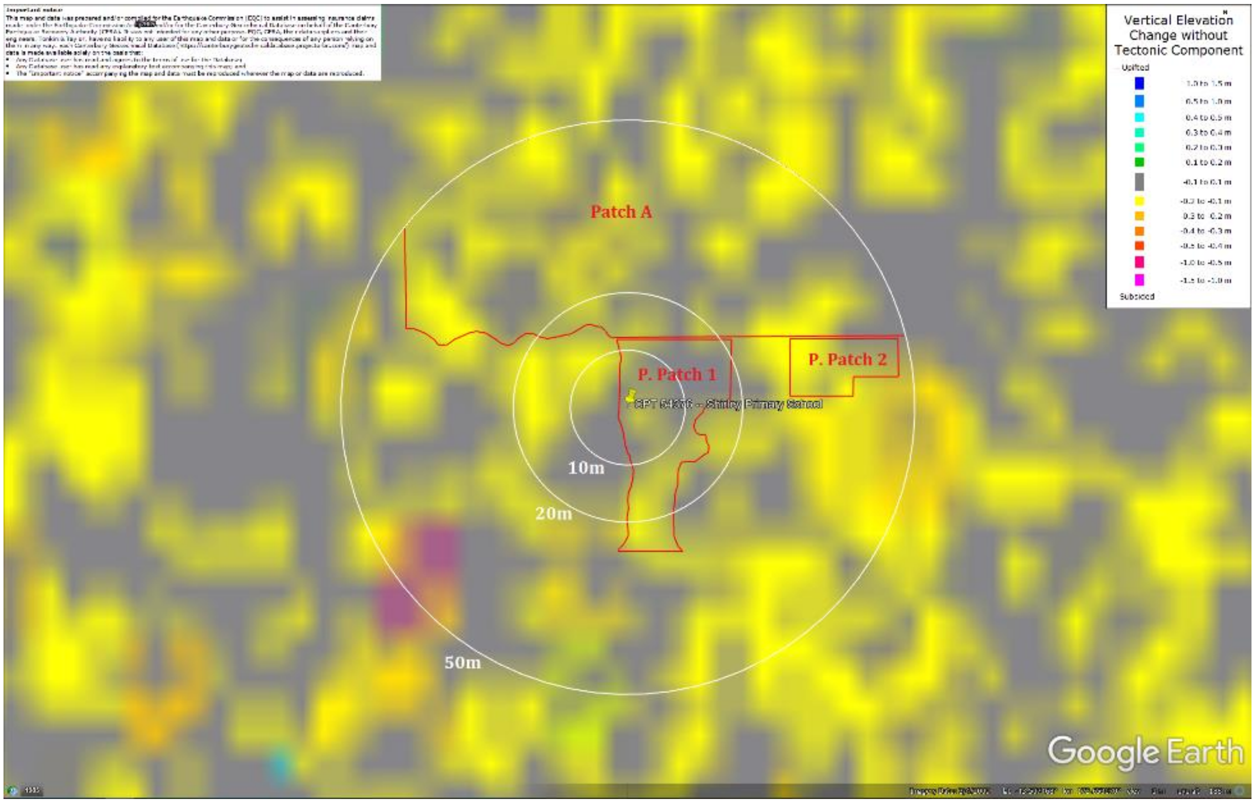

Figure 35: Ground surface subsidence without tectonic component for Sep 2010 Earthquake according to the LiDAR DEM.

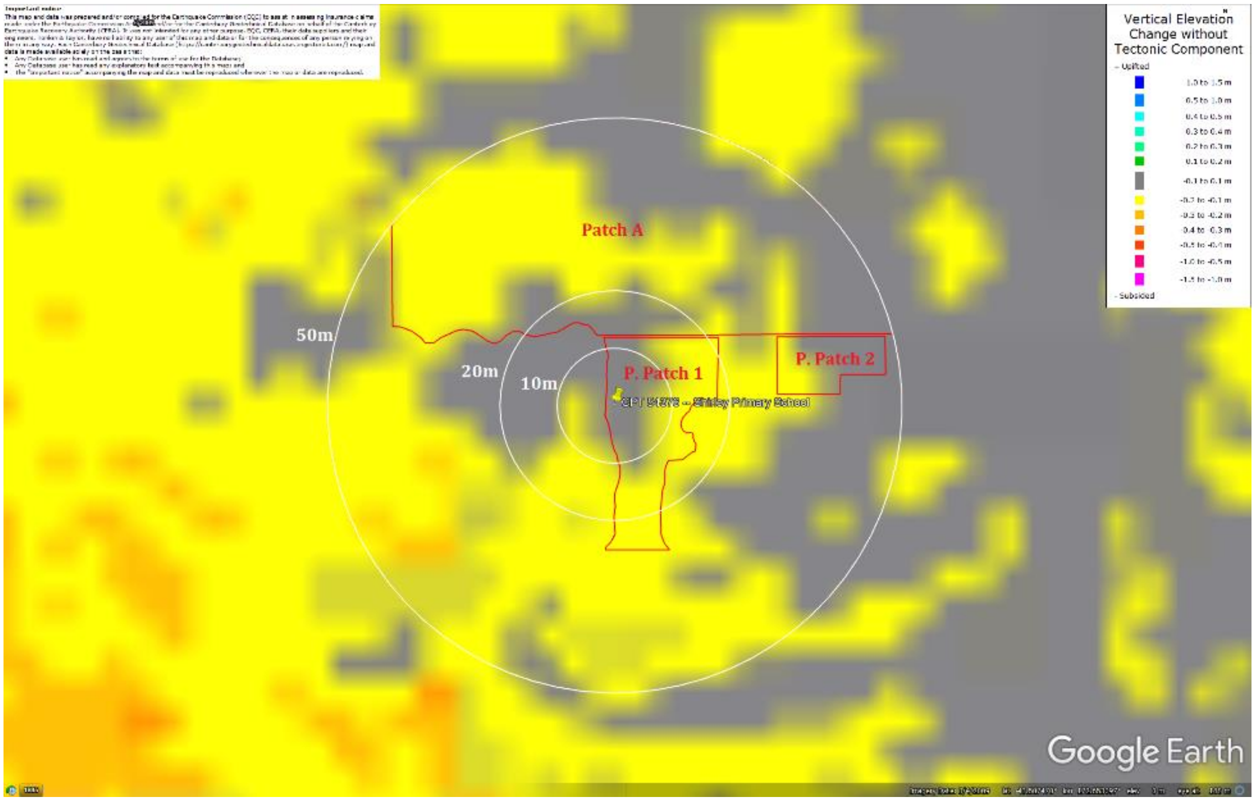

Figure 36: Ground surface subsidence without tectonic component for Feb 2011 Earthquake according to the LiDAR DEM.

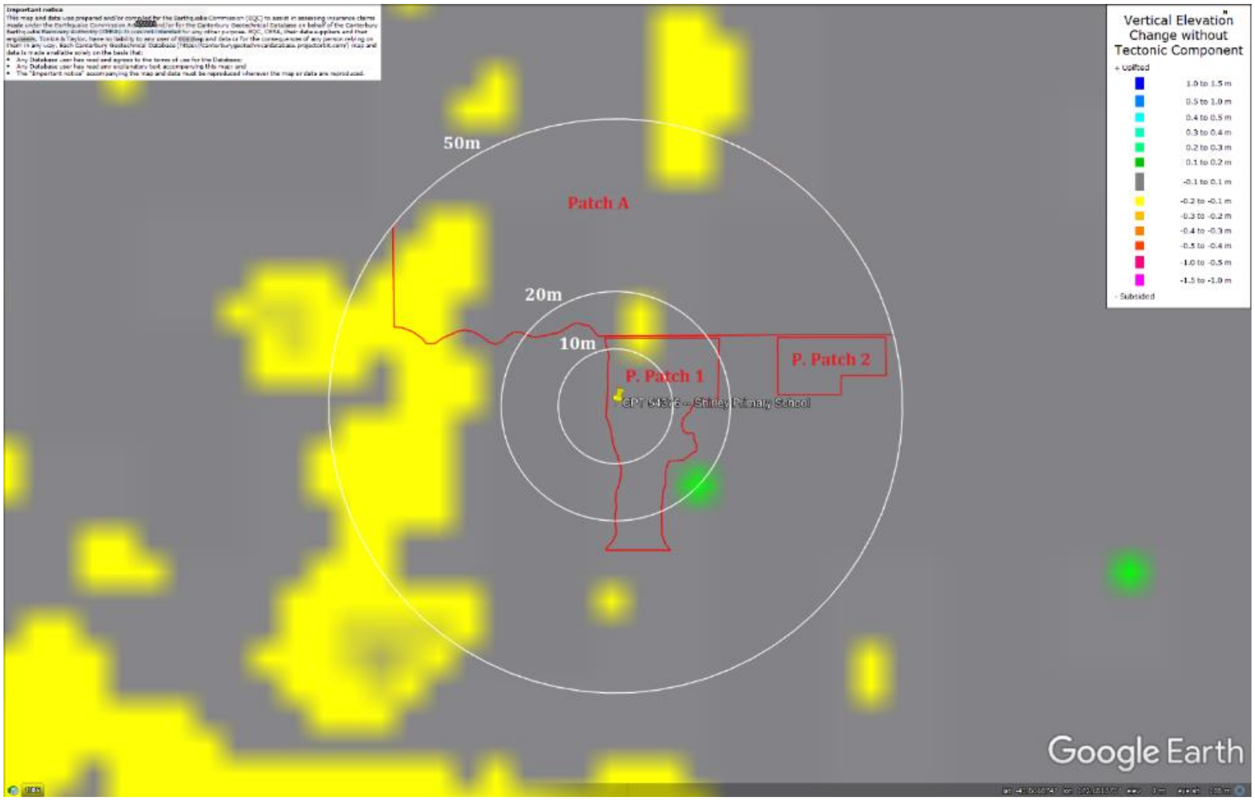

Figure 37: Ground surface subsidence without tectonic component for June 2011 Earthquake according to the LiDAR DEM.

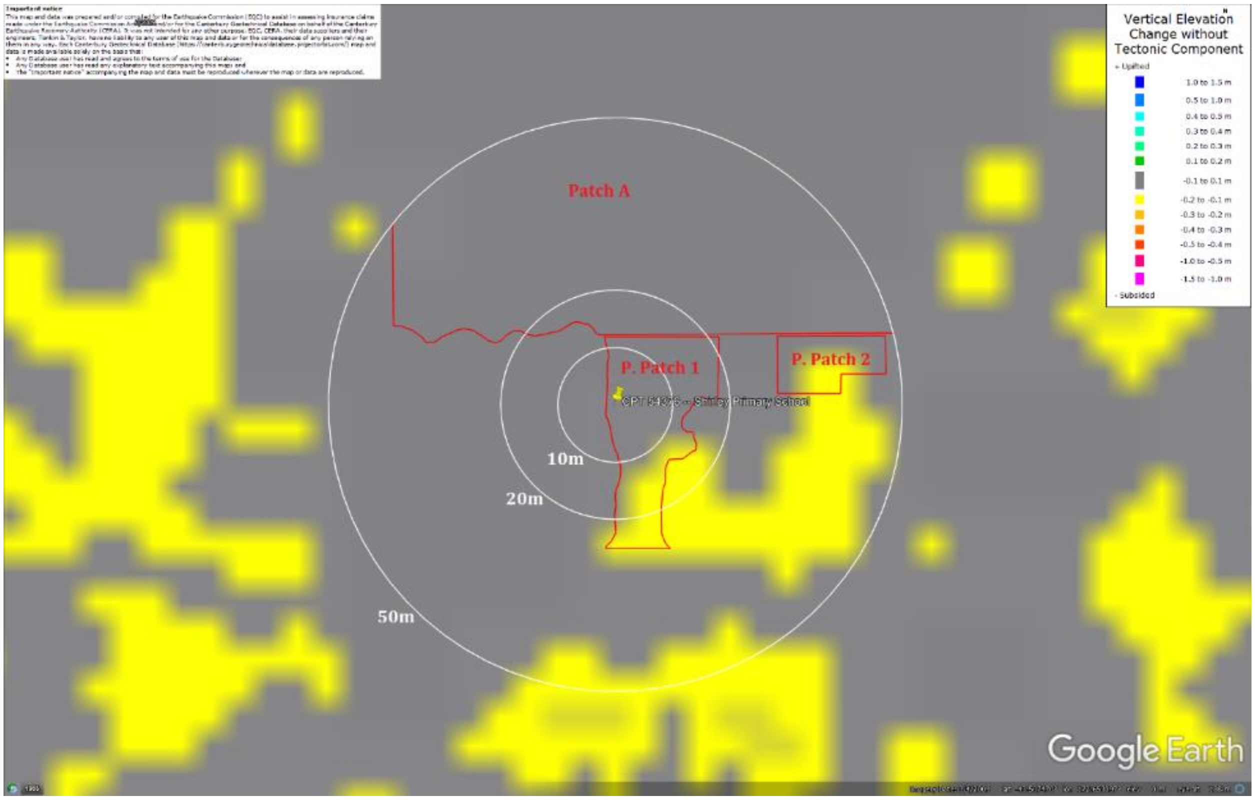

Figure 38: Ground surface subsidence without tectonic component for Dec 2011 Earthquake according to the LiDAR DEM.

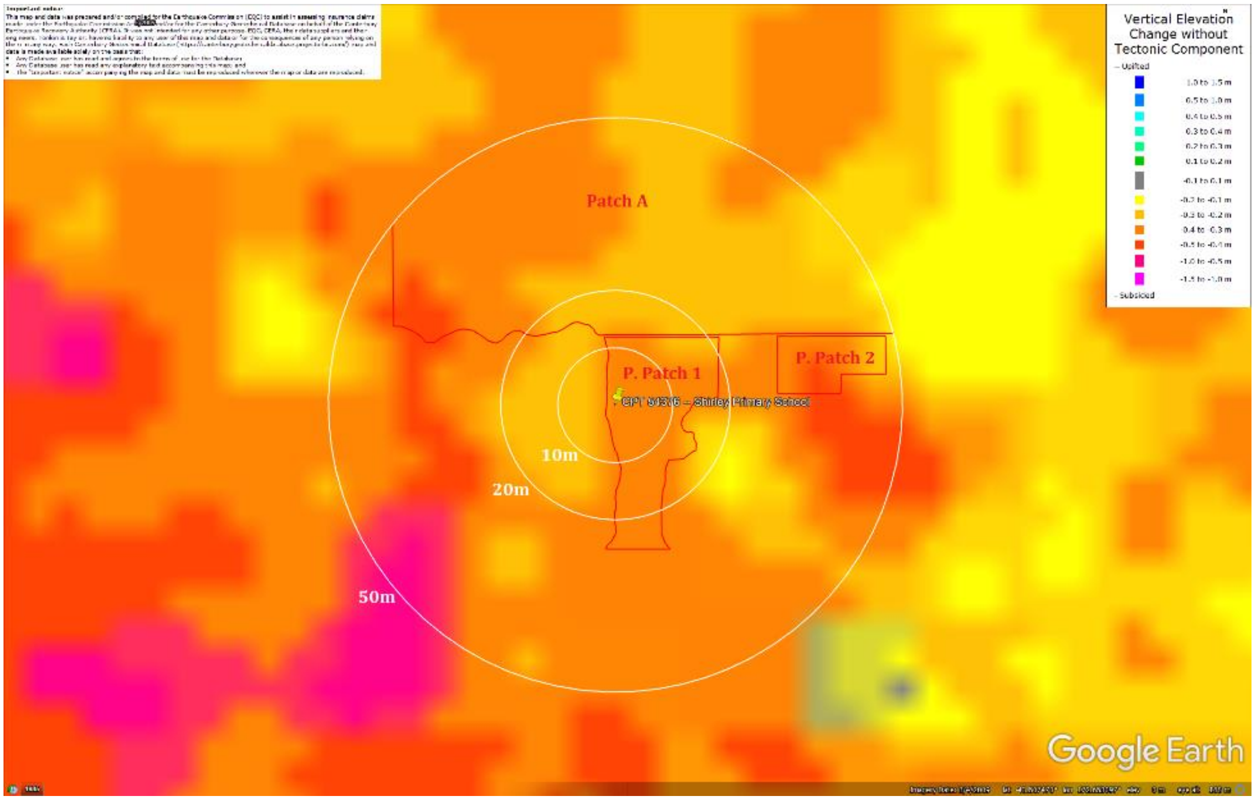

Figure 39: Ground surface subsidence without tectonic component for Canterbury Earthquake Sequence according to the LiDAR DEM.

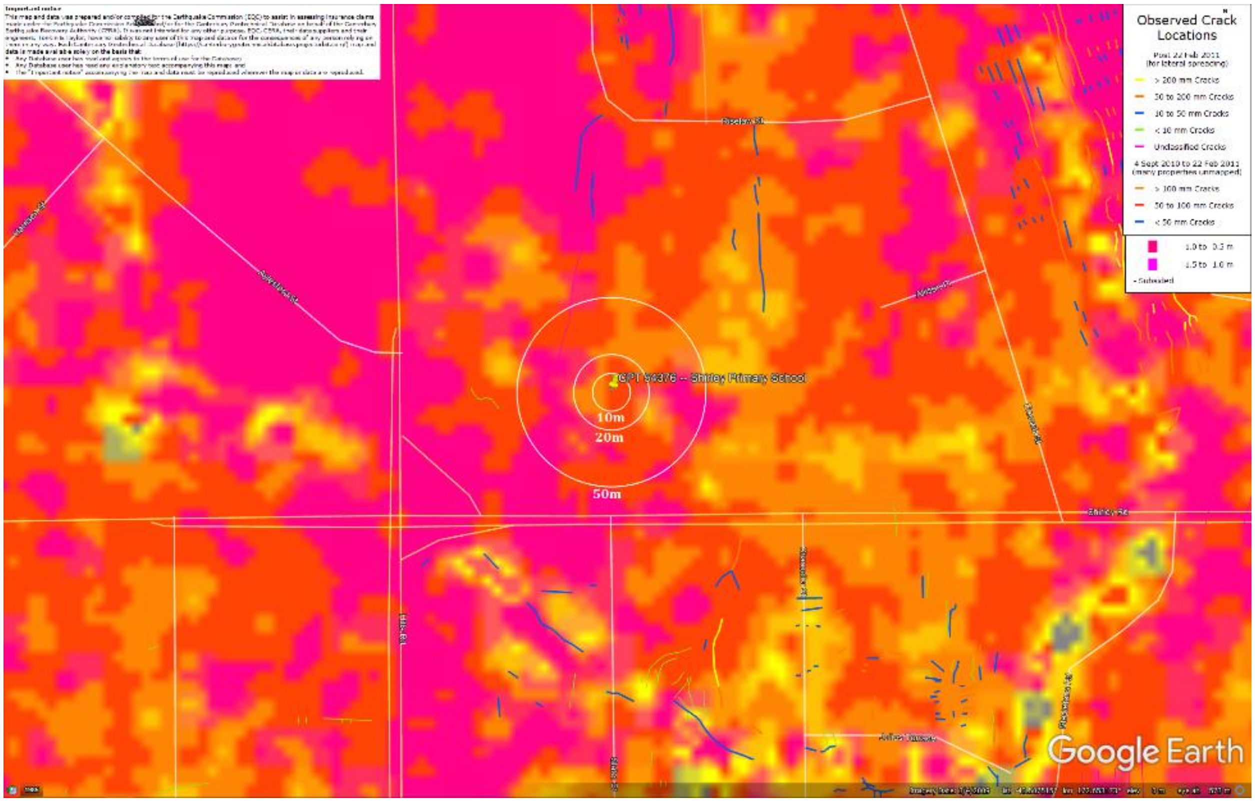

Figure 40: No lateral spreading for Canterbury Earthquake Sequence.

Figure 41: Vertical tectonic movements for Sep 2010 Earthquake.

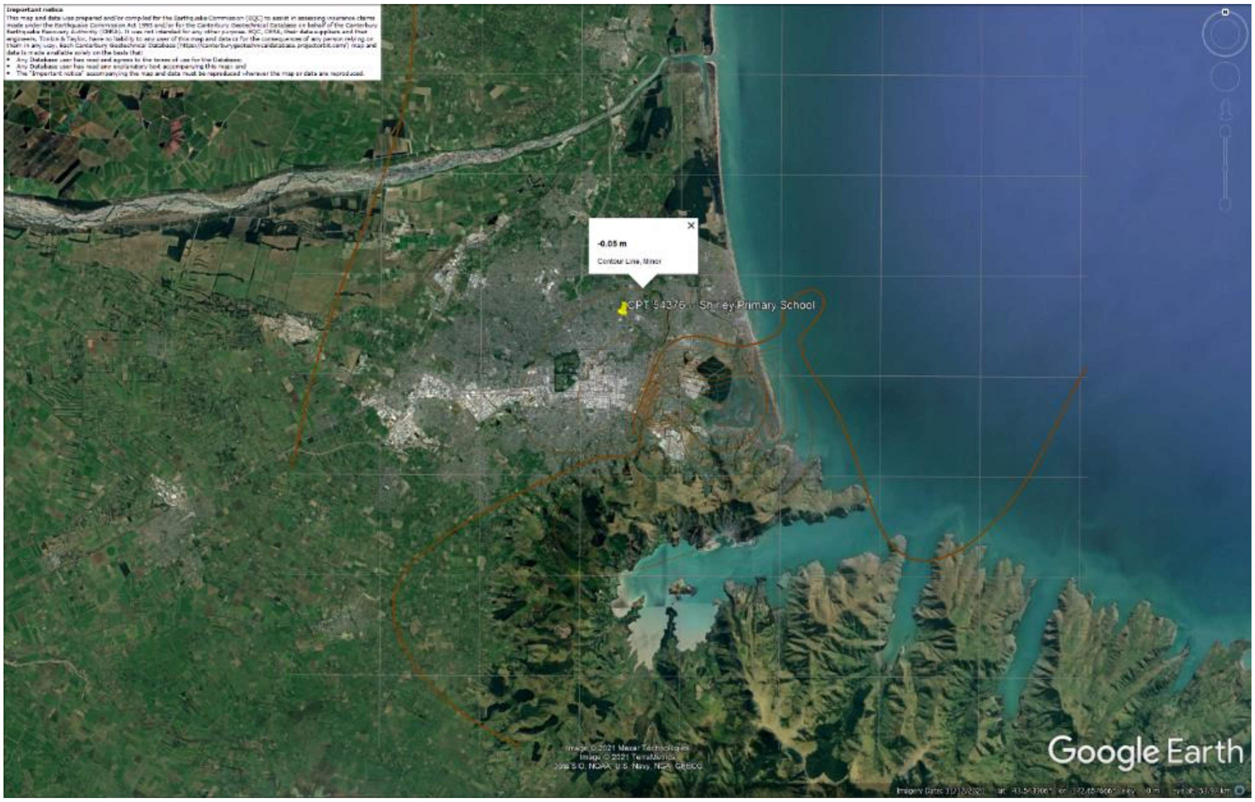

Figure 42: Vertical tectonic movements for Feb 2011 Earthquake.

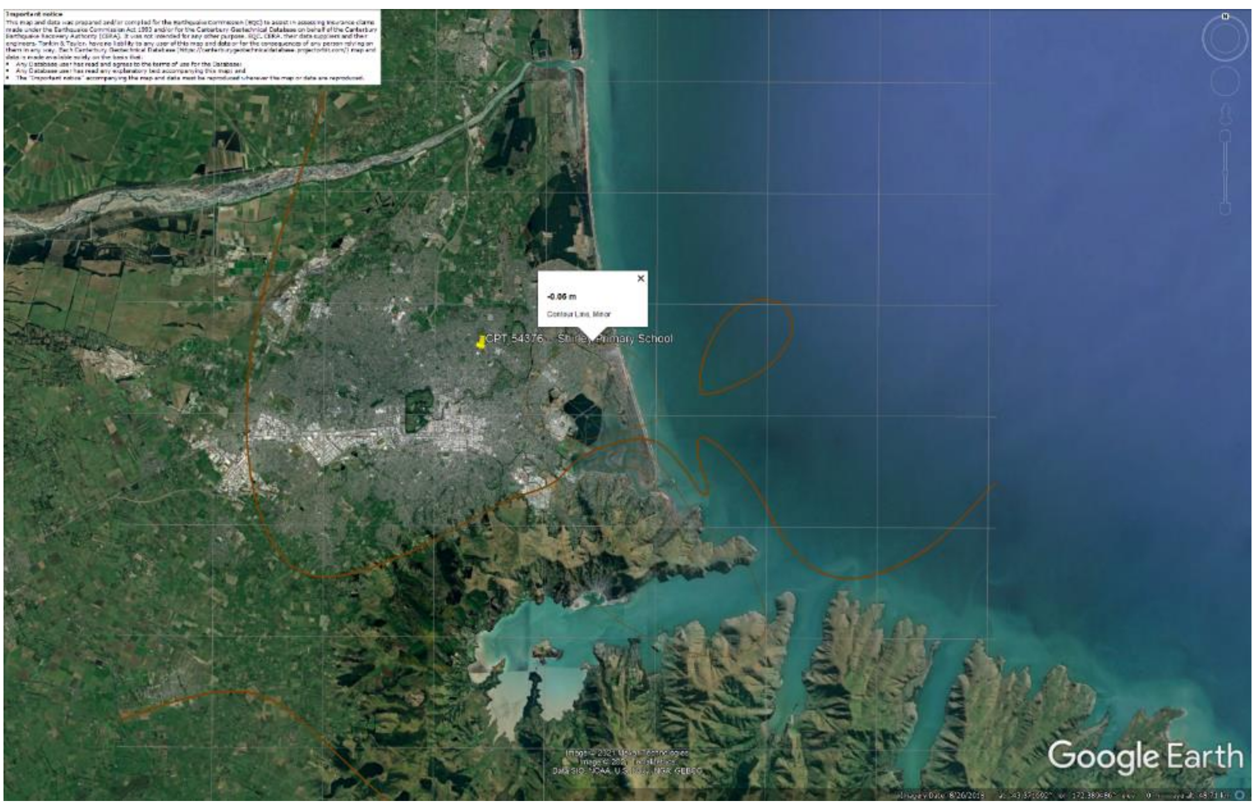

Figure 43: Vertical tectonic movements for June 2011 Earthquake.

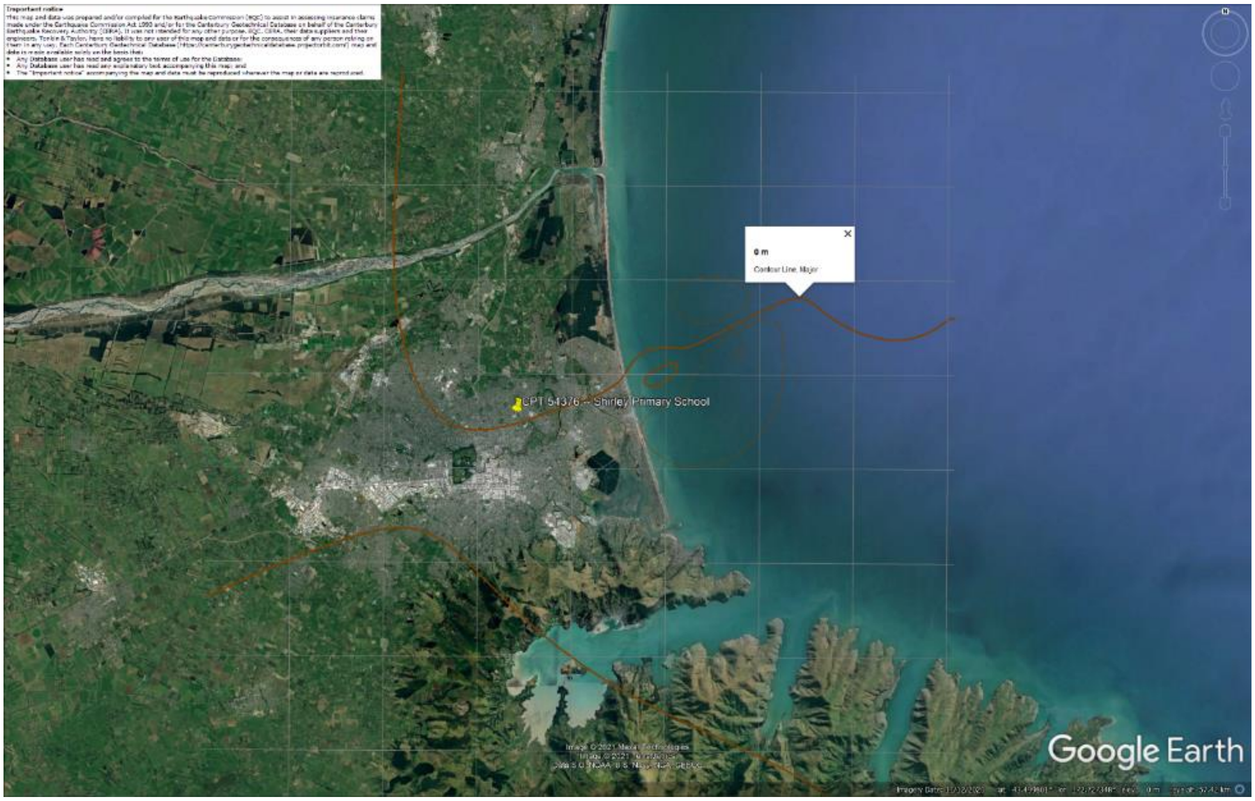

Figure 44: Vertical tectonic movements for Dec 2011 Earthquake.

Figure 45: Vertical tectonic movements for Canterbury Earthquake Sequence.

Figure 46: Sep 5, 2010 LiDAR survey.

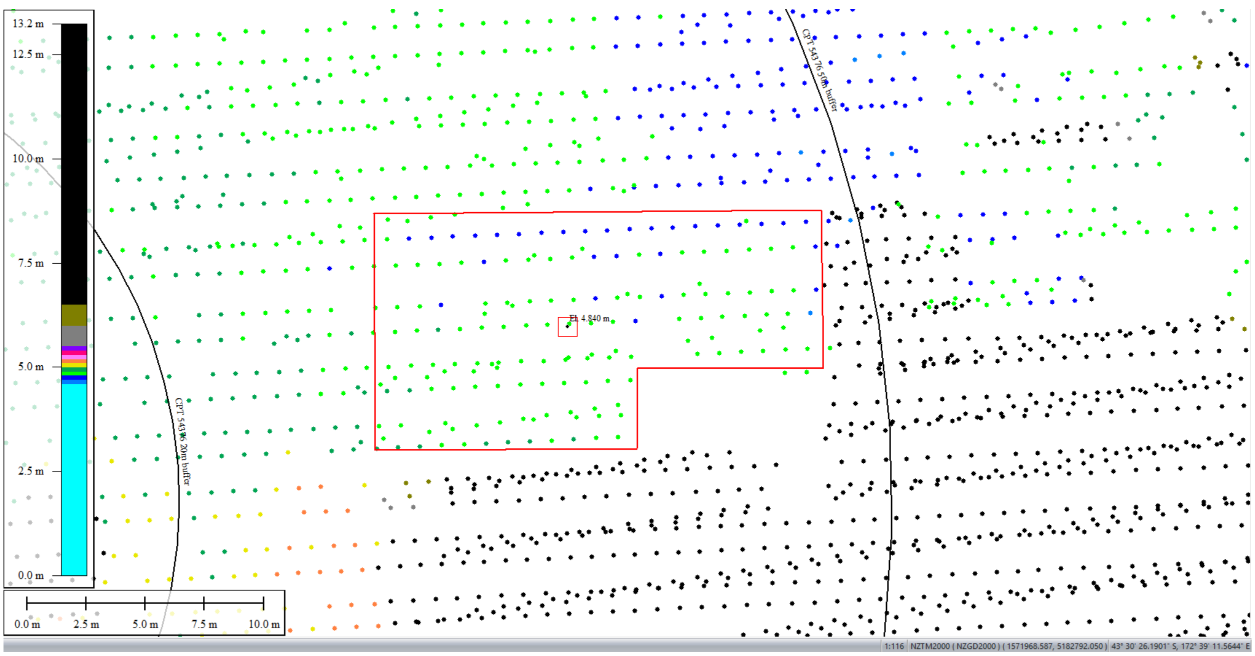

Figure 47: Ground surface elevation averaged over 50-m buffer for P. Patch 2 for Sep 5, 2010 LiDAR survey.

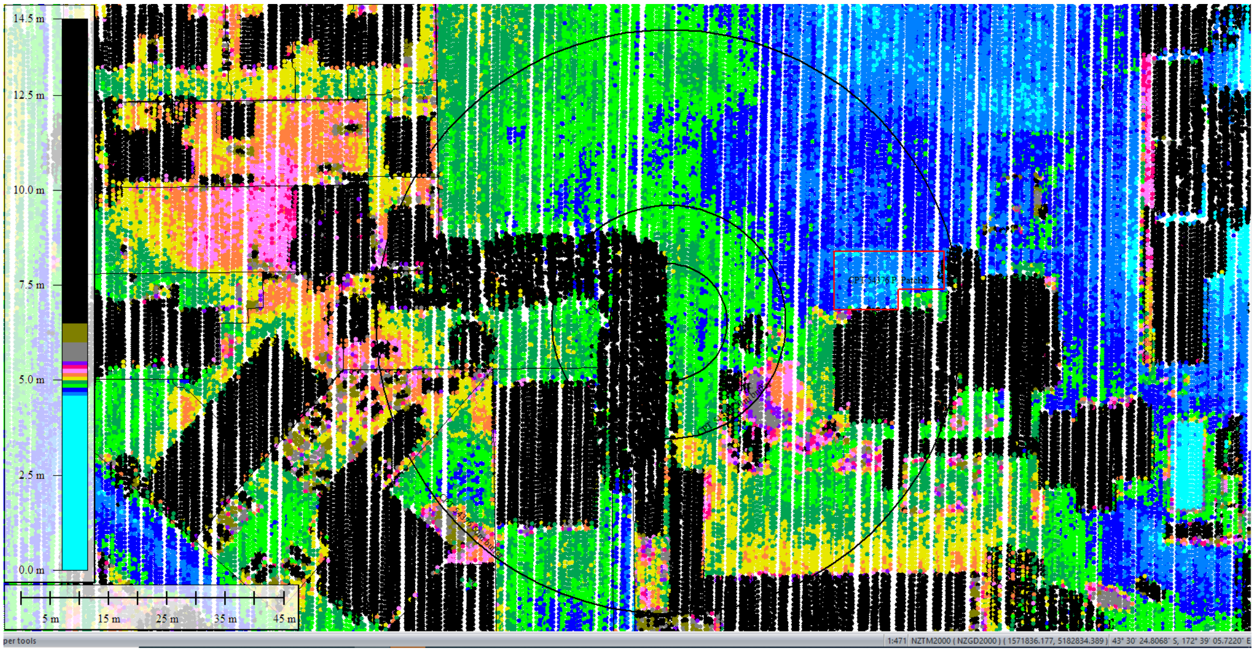

Figure 48: Mar 2011 LiDAR survey.

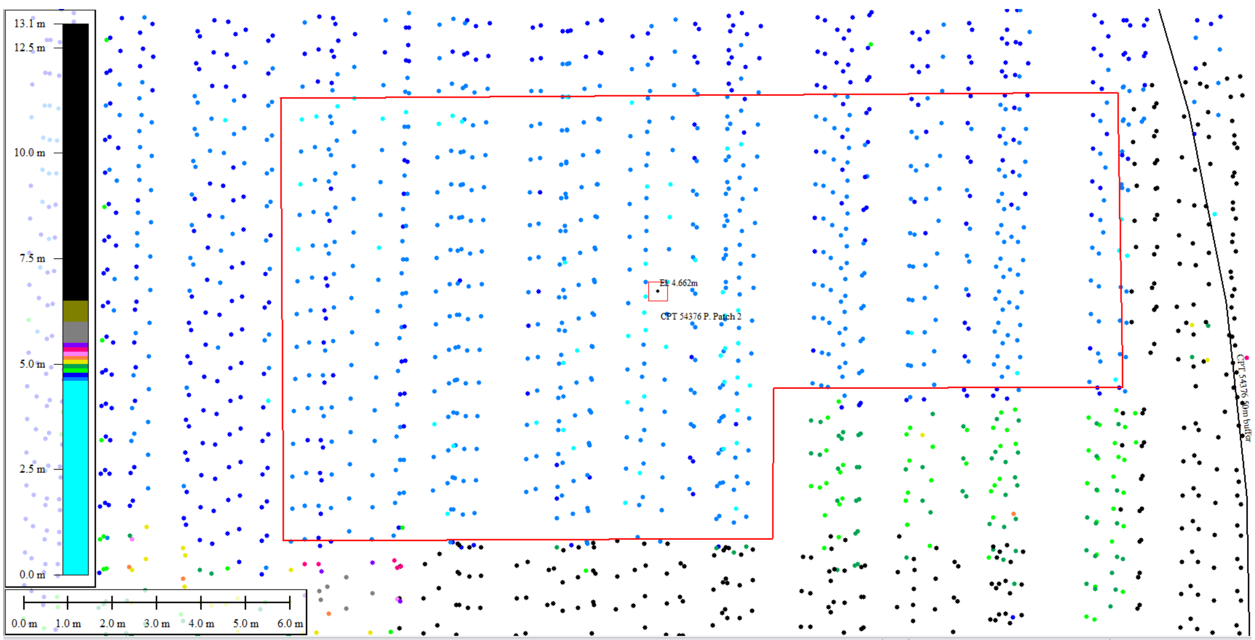

Figure 49: Ground surface elevation averaged over 50-m buffer for P. Patch 2 for Mar 2011 LiDAR survey.

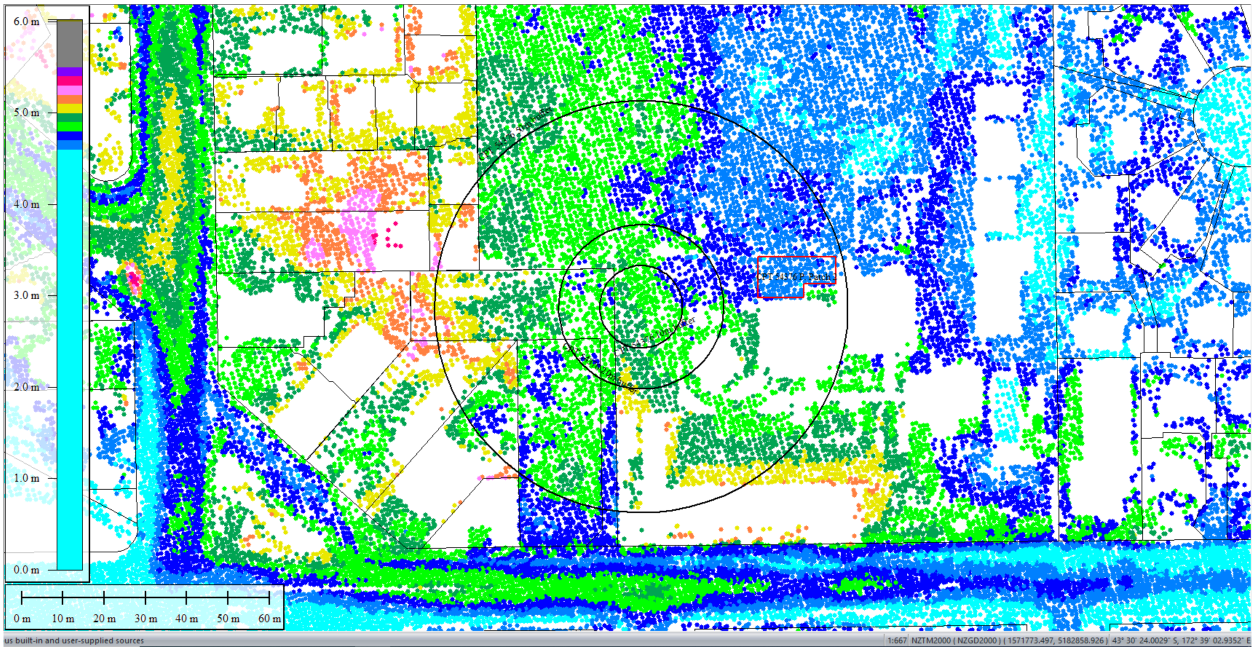

Figure 50: May 2011 LiDAR survey.

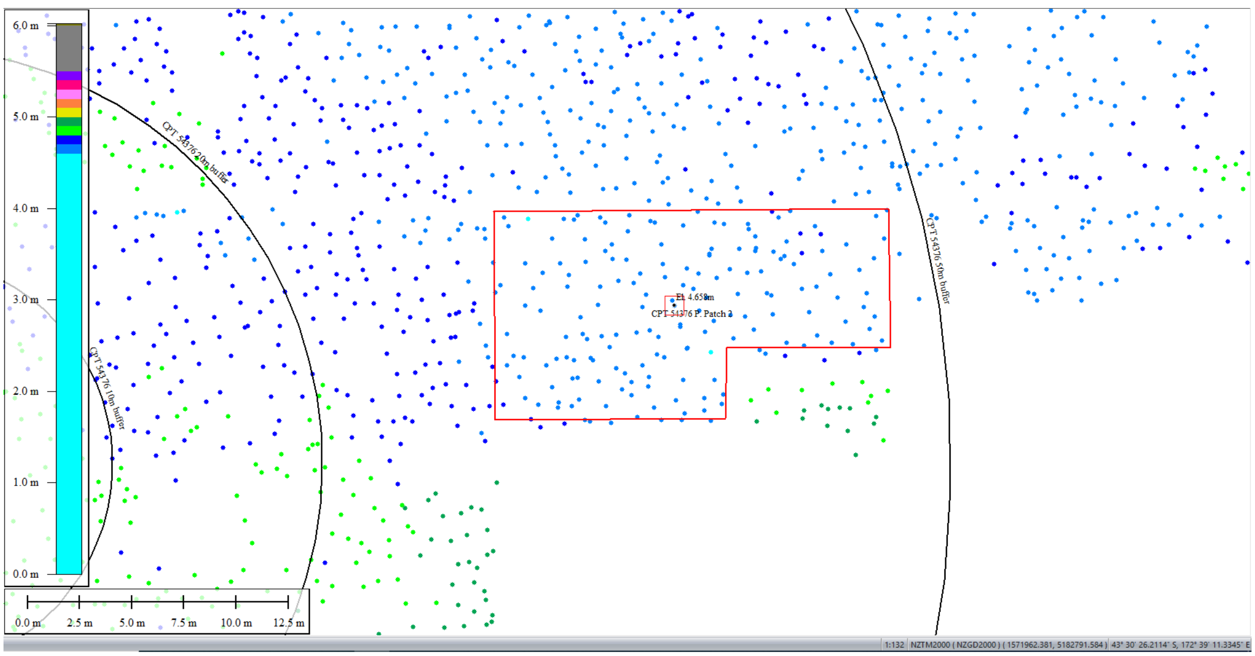

Figure 51: Ground surface elevation averaged over 50-m buffer for P. Patch 2 for May 2011 LiDAR survey.

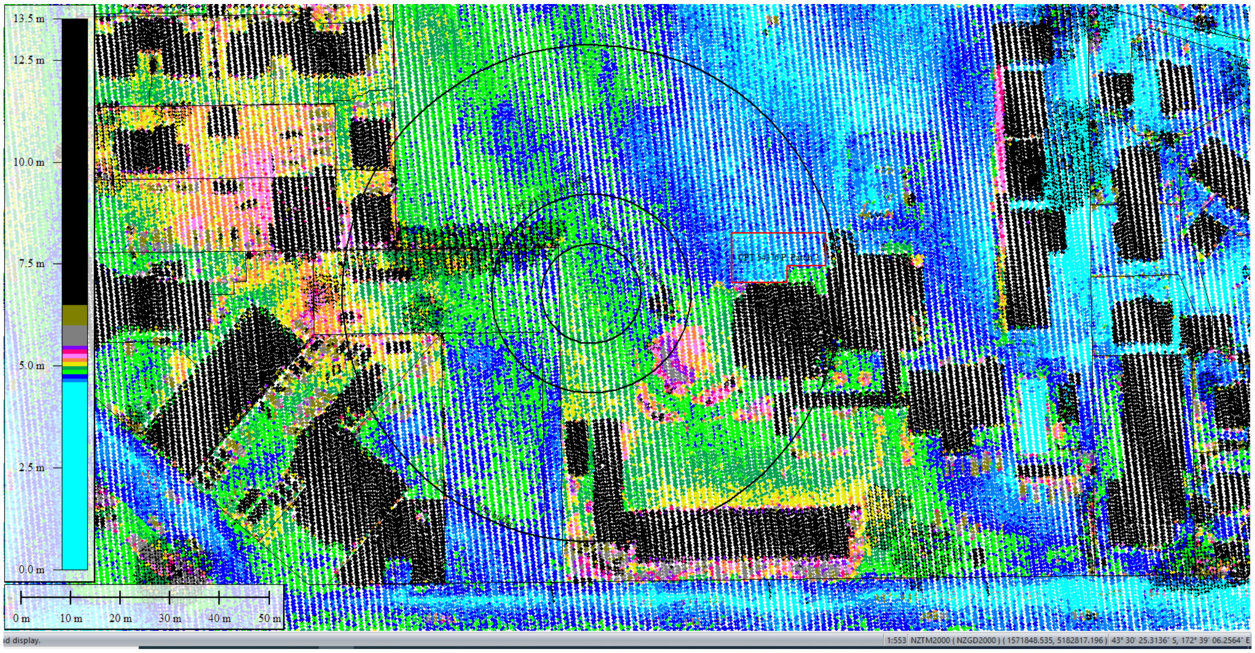

Figure 52: Sep 2011 LiDAR survey.

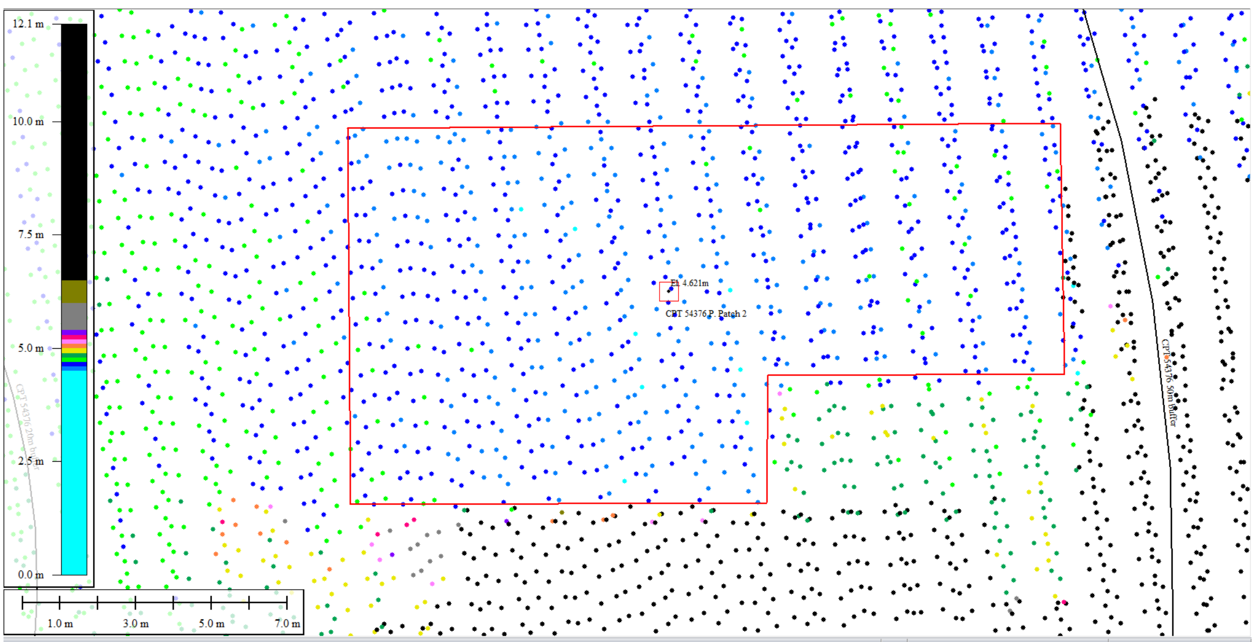

Figure 53: Ground surface elevation averaged over 50-m buffer for P. Patch 2 for Sep 2011 LiDAR survey.

Figure 54: Aerial photograph showing the ejecta outline at the site for Feb-11 EQ.

Figure 55: Aerial photograph acquired on 16 Jun 2011 showing the ejecta outline at the site for Jun-11 EQ.

Figure 56: Ground photographs showing ejecta at nearby properties (19A and 21 Riselaw St; photograph date: May 2011).

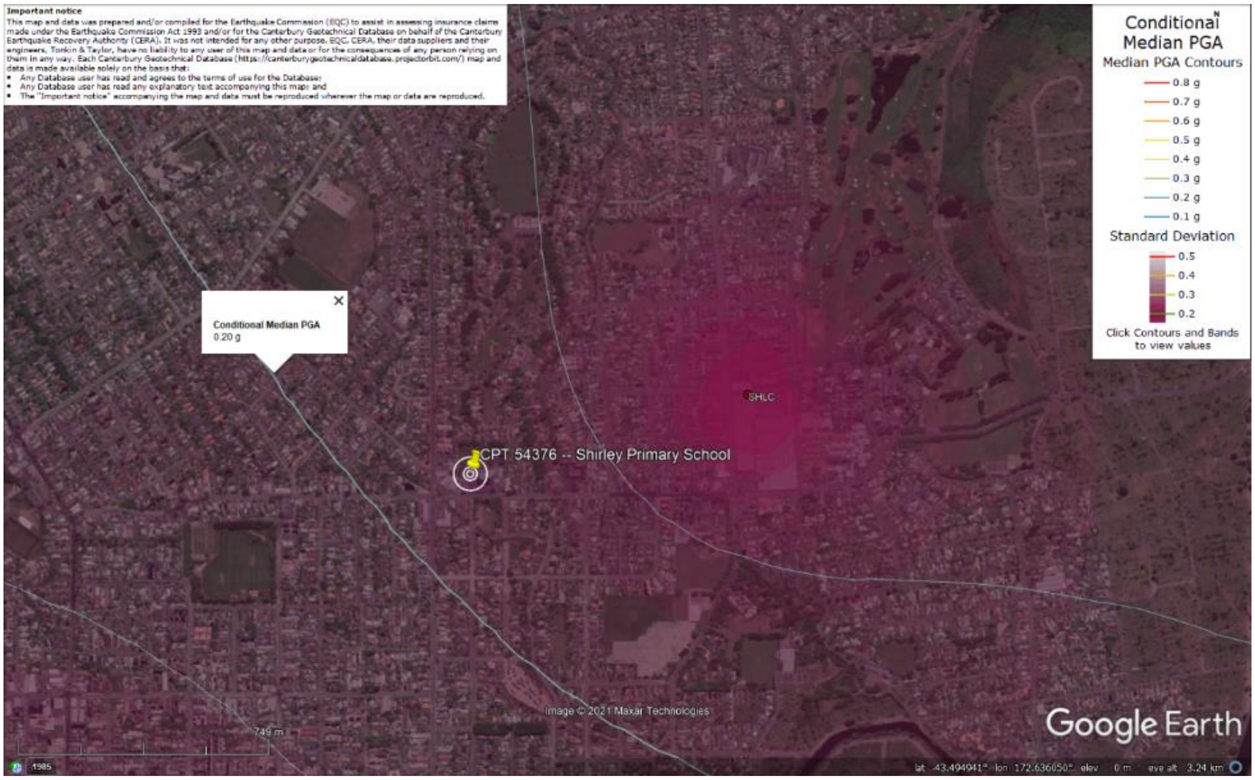

Figure 57: PGA for Sep-10 EQ (st. dev. = 0.275-0.300 ln units).

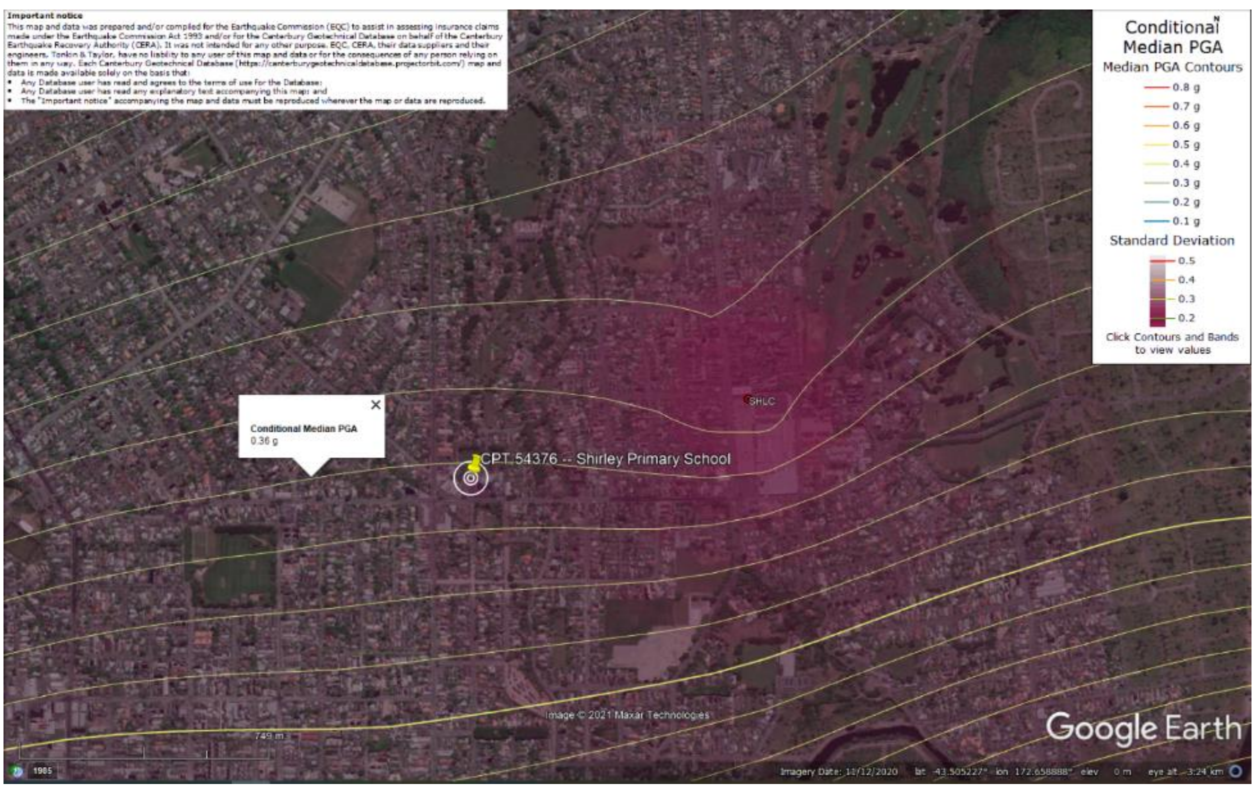

Figure 58: PGA for Feb-11 EQ (st. dev. = 0.300-0.325 ln units).

Figure 59: PGA for Jun-11 EQ (st. dev. = 0.325-0.350 ln units).

Figure 60: PGA for Dec-11 EQ (st. dev. = 0.325-0.350 ln units).

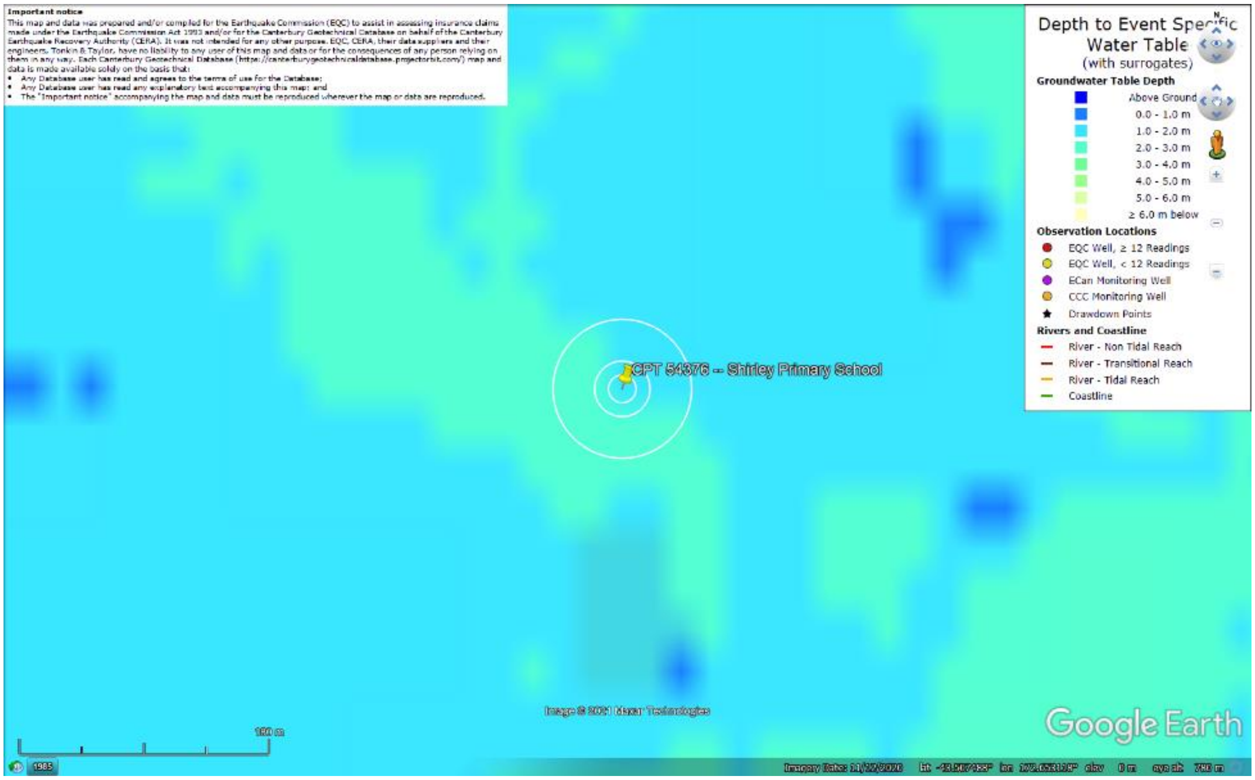

Figure 61: Depth to groundwater table for Sep-10 EQ.

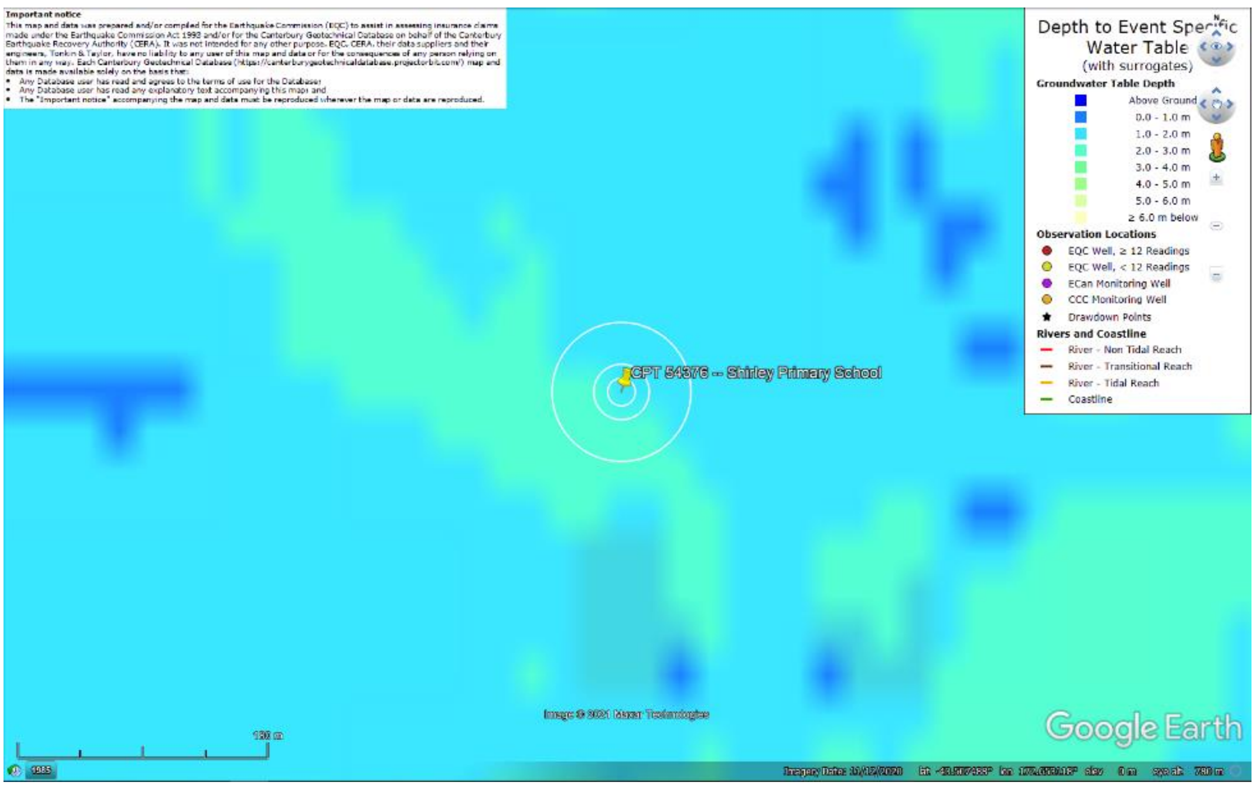

Figure 62: Depth to groundwater table for Feb-11 EQ.

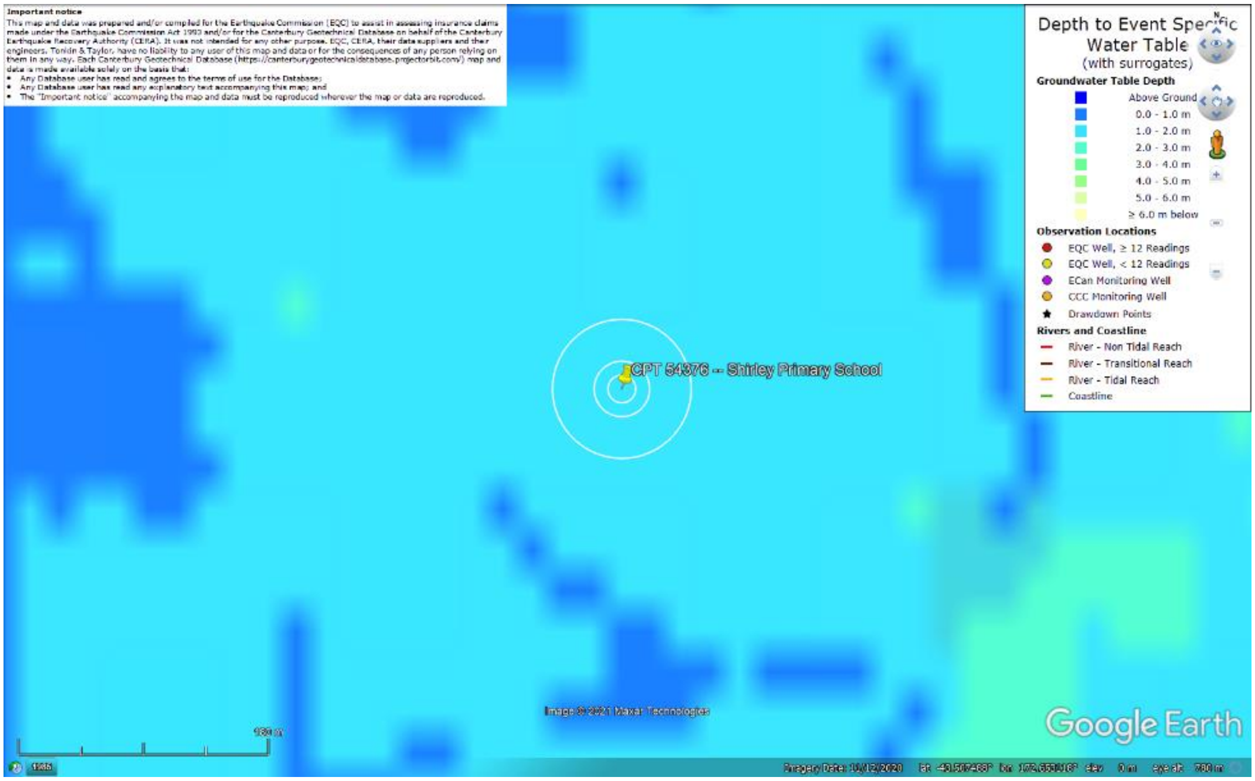

Figure 63: Depth to groundwater table for Jun-11 EQ.

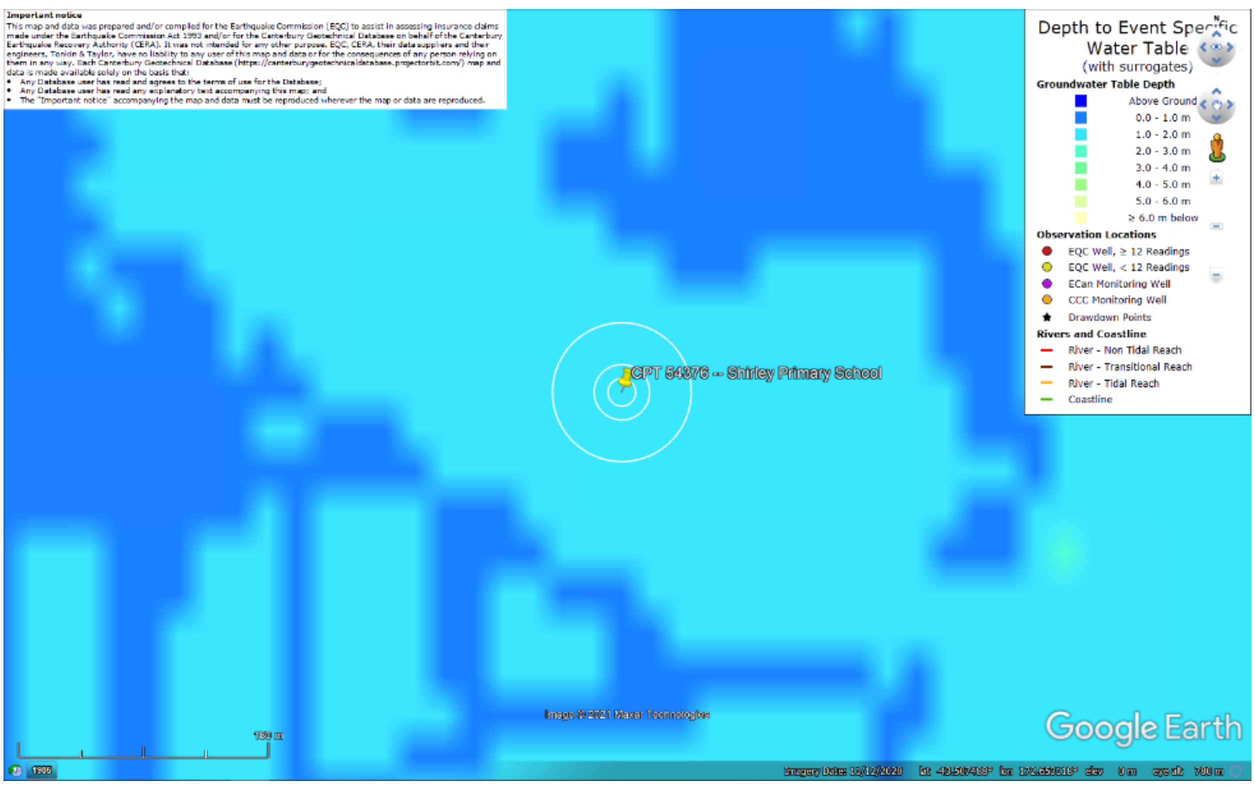

Figure 64: Depth to groundwater table for Dec-11 EQ.

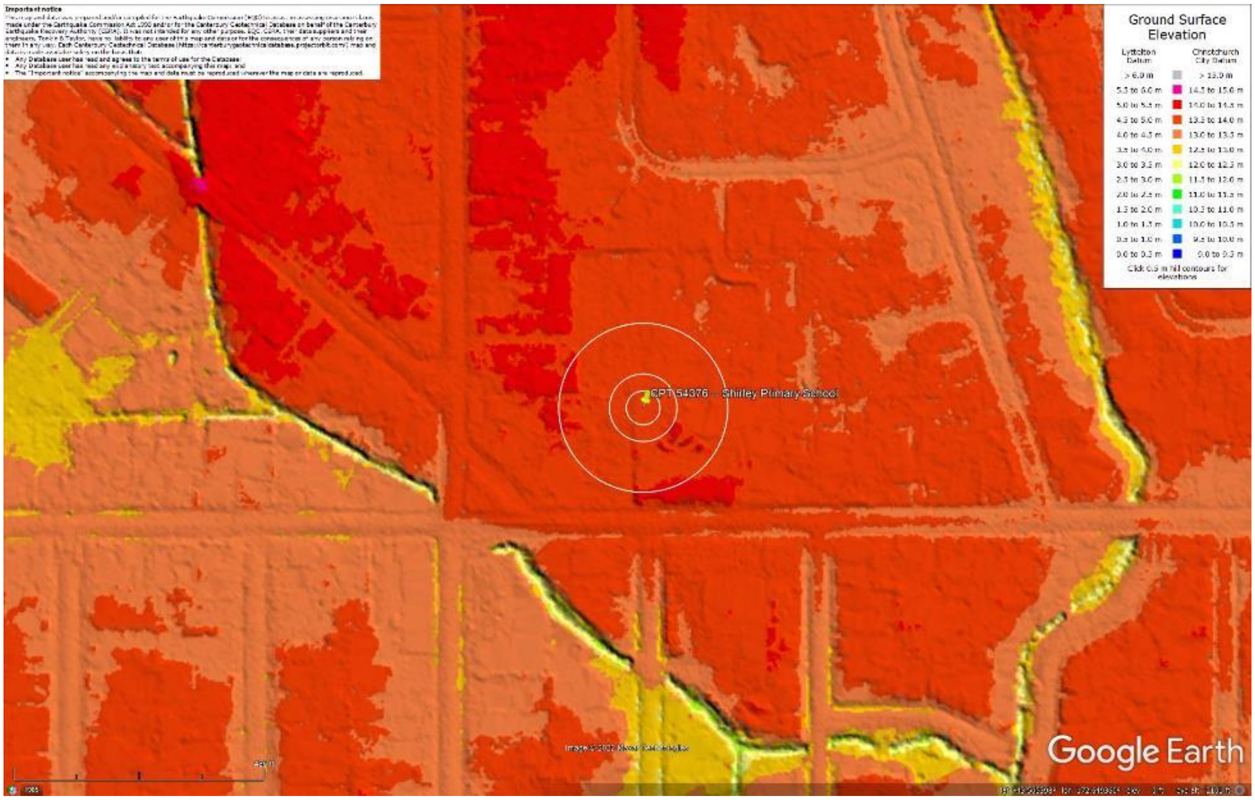

Figure 65: Ground surface elevation (Sep-11 LiDAR survey).

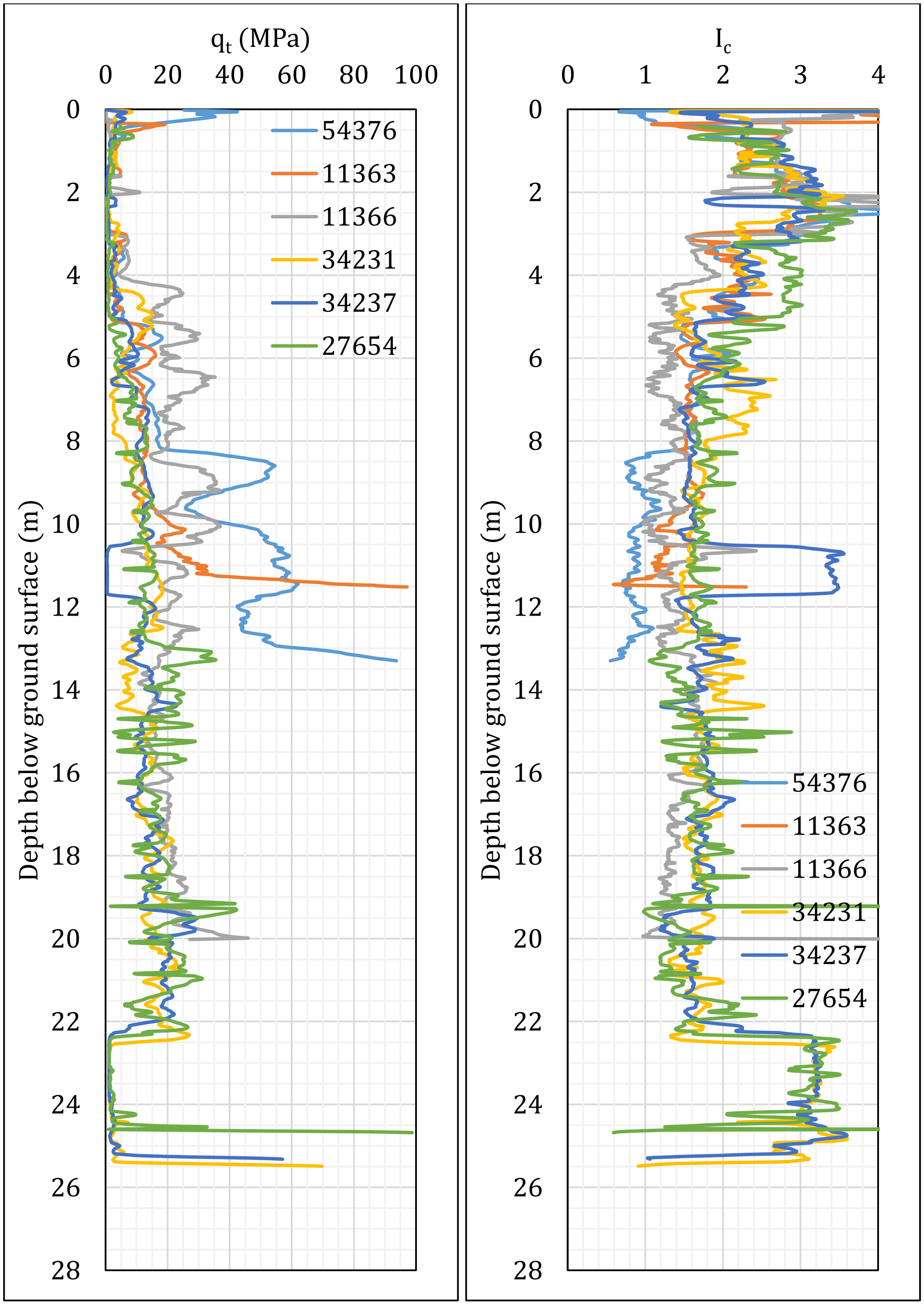

Figure 66: q_t and I_c profiles.

Note 6: The selection of CPTs for the area considered for settlement assessment (Figure 1) is based on the proximity of the CPTs to the considered areas. In accordance with that, the following table shows CPTs that were used for the volumetric settlement analysis in *Cliq v.3.0.3.2*, a CPT soil liquefaction software developed by GeoLogismiki. (The average volumetric settlements were reported in Table 8.)

Table 12: CPT profiles used in volumetric settlement analysis for areas selected for settlement assessment.

CPT ID No.	P. Patch 1 (10-m buffer)	P. Patch 1 (20-m buffer)	P. Patch 1 (50-m buffer)	P. Patch 2	Patch A
54376	✓	✓	✓		✓
11363		✓	✓		
11366				✓	
34231					
34237			✓		
27654					✓

Note: CPTs 11366 and 34237 were used to estimate the average volumetric settlement for CPTs 57436 and 11363 for the depth ranges from 13.3 m to 20 m and from 11.5 m to 20 m, respectively.

Table 13: CPT-based results.

		CPT ID							
EQ Event	Parameter	54376	11363	11366	34231	34237	27654	$\Delta_{13.3m\text{-}20m}$	$\Delta_{11.5m\text{-}20m}$
Sep-10	S_{V1D} (mm)	11	30	6	107	62	62	1	5
	LSN	2	6	1	13	10	7	1	1
	LPI	0	1	0	3	1	2	0	0
	LPI_{ish}	0	0	0	0	1	1	--	--
	$D_{FS<1}$ (m)	undet.	3.96	undet.	3.97	3.82	5.48	--	--
Feb-11	S_{V1D} (mm)	43	90	35	229	187	129	26	36
	LSN	10	18	7	29	28	15	2	3
	LPI	4	9	2	17	14	9	0	1
	LPI_{ish}	1	4	2	6	6	1	--	--
	$D_{FS<1}$ (m)	3.66	2.94	3.02	3.03	2.12	5.44	--	--
Jun-11	S_{V1D} (mm)	11	32	5	82	49	53	0	3
	LSN	2	7	1	12	9	7	0	1
	LPI	0	1	0	2	1	2	0	0
	LPI_{ish}	0	1	0	0	1	1	--	--
	$D_{FS<1}$ (m)	undet.	3.71	undet.	3.95	3.65	5.48	--	--
Dec-11	S_{V1D} (mm)	22	54	10	128	89	76	1	5
	LSN	5	12	2	18	16	10	1	1
	LPI	1	3	0	6	4	3	0	0
	LPI_{ish}	1	0	0	0	0	1	--	--
	$D_{FS<1}$ (m)	3.94	3.34	undet.	3.49	3.53	5.46	--	--

Notes: $D_{FS<1}$ = Depth to the first liquefiable layer (FS_L<1) that is at least 200-mm thick, as determined by the Boulanger and Idriss (2016) liquefaction-triggering procedure (P_L=50%, C_{FC}=0.13, and $I_{c,cutoff}$ =2.6), and exported from *Cliq v.3.0.3.2*; undet. = the specified soil layer was not detected; $\Delta_{13.3m\text{-}20m}$ and $\Delta_{11.5m\text{-}20m}$ indicate the S_{V1D}, LSN, and LPI values that were added to CPTs 54376 and 11363, respectively, due to their penetration depths <20 m.

Note 7: Based on the borehole log (BH 11359, Figure 1), the soil profile consists of the (1) gravelly fill below the 50-mm thick concrete pavement to a depth of 0.3 m, (2) sandy silt, SM, to a depth of 1.9 m, (3) peat, Pt, to a depth of 2 m, (4) organic silt, OM, to a depth of 2.6 m, (5) sandy silt, ML, to a depth of 3.5 m, (6) silty sand, SM, to a depth of 5.2 m, (7) fine to medium sand, SP, to a depth of 9.4 m, (8) gravelly fine to coarse sand, SW, to a depth of 10.05 m, (9) sandy fine to coarse gravel, GW, to a depth of 10.50 m, (10) gravelly fine to coarse sand, SW, to a depth of 11.0 m, (11) Sandy fine to coarse gravel, SW, to a depth of 11.25 m, (12) fine to coarse sand, SP, to a depth of 12.5 m, (13) gravelly fine to coarse sand, SW, to a depth of 13.9 m, (14) sandy fine to medium gravel, GW, to a depth of 14.4 m, (15) fine to medium sand, SP, to a depth of 14.7 m, (16) sandy fine to medium gravel, GW, to a depth of 15.4 m, (17) gravelly fine to coarse sand, SW, to a depth of 16 m, (18) fine to medium sand, SP, to a depth of 18.4 m, (19) sandy fine to medium gravel, GW, to a depth of 19.1 m, and (20) gravelly fine to medium sand, SW, to a depth of 19.95 m. Based on the borehole log BH 27656 (Figure 1), the groundwater table is at a depth of 1.5 m below the ground surface. In addition, the nearby borehole logs, it is estimated that the soil layers up to a depth of 11.3 m are the Yaldhurst members of the Springston formation, whereas the soil layers below 11.3 m are of the Christchurch formation.

Note 8: The ejecta-induced free-field settlement provided in Table 11 is an areal average settlement due to ejecta, which is based on the total settlement assessment area, A_T (provided in Table 9 and repeated in Table 14). However, the considered area was not always covered completely with ejecta; thus, it is important to provide the localized ejecta-induced settlement, too. The localized settlement due to ejecta is estimated using photographic evidence only as

$$S_{E,P\_localized} = \frac{V_E}{A_E}$$

where V_E is the total volume of ejecta within A_T and A_E is the total coverage area of ejecta within A_T. Please note that the areal ejecta-induced settlement provided in Table 14 as S_{E,P_areal} is the same as $S_{E,P}$ in Table 11, which was estimated as

$$S_{E,P\_areal} = S_{E,P} = \frac{V_E}{A_T}$$

where V_E is the total volume of ejecta within A_T and A_T is the total settlement assessment area.

Table 14a: Areal and localized ejecta-induced settlement estimates for P. Patch 1 (10-m buffer) based on photographic evidence.

Earthquake Event	A_T (m²)	A_E (m²)	V_E (m³)	S_{E,P_areal} (mm)	$S_{E,P\_localized}$ (mm)
Sep-10	117	0	0	0	0
Feb-11	117	117	5.5-10.0	65±20	65±20
Jun-11	153	61.3	1.5-2.8	15±5	35±10
Dec-11	117	0	0	0	0

Notes: S_{E,P_areal} = $S_{E,P}$ reported in Table 11 = areal ejecta-induced settlement; $S_{E,P\_localized}$ = localized ejecta-induced settlement; A_T = total settlement assessment area; V_E = total volume of ejecta within A_T; A_E = total area of ejecta within A_T; The estimates of both areal and localized ejecta-induced settlement are rounded to the nearest 5; Final plus/minus values are also rounded to the nearest 5.

Table 14b: Areal and localized ejecta-induced settlement estimates for P. Patch 1 (20-m buffer) based on photographic evidence.

Earthquake Event	A_T (m^2)	A_E (m^2)	V_E (m^3)	S_{E,P_areal} (mm)	$S_{E,P\_localized}$ (mm)
Sep-10	348	0	0	0	0
Feb-11	348	348	17.5-32.8	70±20	70±20
Jun-11	357	219	5.9-11.2	25±5	40±10
Dec-11	348	0	0	0	0

Notes: S_{E,P_areal} = $S_{E,P}$ reported in Table 11 = areal ejecta-induced settlement; $S_{E,P\_localized}$ = localized ejecta-induced settlement; A_T = total settlement assessment area; V_E = total volume of ejecta within A_T; A_E = total area of ejecta within A_T; The estimates of both areal and localized ejecta-induced settlement are rounded to the nearest 5; Final plus/minus values are also rounded to the nearest 5.

Table 14c: Areal and localized ejecta-induced settlement estimates for P. Patch 1 (50-m buffer) based on photographic evidence.

Earthquake Event	A_T (m^2)	A_E (m^2)	V_E (m^3)	S_{E,P_areal} (mm)	$S_{E,P\_localized}$ (mm)
Sep-10	391	0	0	0	0
Feb-11	391	391	20.1-37.8	75±25	75±25
Jun-11	391	244	6.6-12.5	25±5	40±10
Dec-11	391	0	0	0	0

Notes: S_{E,P_areal} = $S_{E,P}$ reported in Table 11 = areal ejecta-induced settlement; $S_{E,P\_localized}$ = localized ejecta-induced settlement; A_T = total settlement assessment area; V_E = total volume of ejecta within A_T; A_E = total area of ejecta within A_T; The estimates of both areal and localized ejecta-induced settlement are rounded to the nearest 5; Final plus/minus values are also rounded to the nearest 5.

Table 14d: Areal and localized ejecta-induced settlement estimates for Patch A (50-m buffer) based on photographic evidence.

Earthquake Event	A_T (m^2)	A_E (m^2)	V_E (m^3)	S_{E,P_areal} (mm)	$S_{E,P\_localized}$ (mm)
Sep-10	2519	0	0	0	0
Feb-11	2519	1270	164-246	80±15	160±30
Jun-11	2531	359	22.1-39.1	15±5	85±25
Dec-11	2519	0	0	0	0

Notes: S_{E,P_areal} = $S_{E,P}$ reported in Table 11 = areal ejecta-induced settlement; $S_{E,P\_localized}$ = localized ejecta-induced settlement; A_T = total settlement assessment area; V_E = total volume of ejecta within A_T; A_E = total area of ejecta within A_T; The estimates of both areal and localized ejecta-induced settlement are rounded to the nearest 5; Final plus/minus values are also rounded to the nearest 5.

Table 14e: Areal and localized ejecta-induced settlement estimates for P. Patch 2 (50-m buffer) based on photographic evidence.

Earthquake Event	A_T (m^2)	A_E (m^2)	V_E (m^3)	S_{E,P_areal} (mm)	$S_{E,P\_localized}$ (mm)
Sep-10	166	0	0	0	0
Feb-11	166	166	3.3-5.7	25±5	25±5
Jun-11	166	39.9	0.3-0.8	5±5	15±5
Dec-11	166	0	0	0	0

Notes: S_{E,P_areal} = $S_{E,P}$ reported in Table 11 = areal ejecta-induced settlement; $S_{E,P\_localized}$ = localized ejecta-induced settlement; A_T = total settlement assessment area; V_E = total volume of ejecta within A_T; A_E = total area of ejecta within A_T; The estimates of both areal and localized ejecta-induced settlement are rounded to the nearest 5; Final plus/minus values are also rounded to the nearest 5.

<u>Summary 2:</u>

- **The best estimate of the localized ejecta-induced free-field ground settlement of the unpaved surface at the Shirley Primary School site for the SEP 2010, FEB 2011, JUN 2011, and DEC 2011 earthquake is 0 mm, 160±30 mm, 85±25 mm, and 0 mm, respectively.**
- **The best estimate of the localized ejecta-induced free-field ground settlement of the paved surface at the Shirley Primary School site for the SEP 2010, FEB 2011, JUN 2011, and DEC 2011 earthquake is 0 mm, 75±25 mm, 40±10 mm, and 0 mm, respectively.**